Zoological Journal of the Linnean Society, 2007, **149**, 533–567. With 9 figures

Cranial osteology and phylogenetic relationships of *Hamadasuchus rebouli* (Crocodyliformes: Mesoeucrocodylia) from the Cretaceous of Morocco

HANS C. E. LARSSON[1]* and HANS-DIETER SUES[2] FLS

[1]*Redpath Museum, McGill University, 859 Sherbrooke Street W., Montréal, QC H3A 2K6, Canada*
[2]*National Museum of Natural History, Smithsonian Institution, NHB MRC 106, PO Box 37012, Washington, DC 20013–7012, USA*

Received February 2005; accepted for publication June 2006

This paper presents a detailed description of the skull and part of the mandible of the crocodyliform reptile *Hamadasuchus rebouli* from the Kem Kem beds (Upper Cretaceous: Albian–Cenomanian) of south-eastern Morocco. This taxon of deep-snouted ziphodont crocodyliform can be diagnosed by a number of autapomorphies. Phylogenetic analysis of a diverse array of crocodylomorph taxa found strong support for a clade comprising *H. rebouli*, Peirosauridae, and *Sebecus*. The name **Sebecia nom. nov.** is proposed for this grouping, which is diagnosed by numerous characters, including the participation of the quadratojugal in the mandibular condyle. The distribution of this diverse and long-lived clade lends further support to the biogeographical hypothesis that faunal connections existed between Africa and South America well into mid-Cretaceous times. © 2007 The Linnean Society of London, *Zoological Journal of the Linnean Society*, 2007, **149**, 533–567.

ADDITIONAL KEYWORDS: Crocodylomorpha – Hamadasuchus – skull.

INTRODUCTION

The evolutionary history of Mesozoic crocodyliform reptiles from Africa is still poorly understood. Most of the relatively few forms known to date are Cretaceous in age. Stromer (1914, 1925, 1933, 1936) described a series of crocodyliform taxa from the Upper Cretaceous (Cenomanian) of the Bahariya Oasis in the Western Desert of Egypt. Most noteworthy among these are *Libycosuchus brevirostris* (Stromer, 1914; Buffetaut, 1976b) and the huge, 'duck-billed' *Stomatosuchus inermis* (Stromer, 1925, 1936; the holotype was destroyed during World War II). Early Cretaceous strata in Niger have also yielded assemblages of crocodyliform reptiles, including the giant pholidosaurid *Sarcosuchus imperator* (de Broin & Taquet, 1966; Taquet, 1976; Buffetaut & Taquet, 1977; Buffetaut, 1981b; Sereno *et al*., 2001), the enigmatic *Trematochampsa taqueti* (Buffetaut, 1974, 1976a), the smaller *Araripesuchus wegeneri* (Buffetaut & Taquet, 1979; Buffetaut, 1981a; Ortega *et al*., 2000; referred to *Hamadasuchus* by Prasad & Lapparent de Broin, 2002), the longirostrine *Stolokrosuchus lapparenti* (Larsson, 2000; Larsson & Gado, 2000), and the small notosuchian *Anatosuchus minor* (Sereno *et al*., 2003). Furthermore, several crocodyliform taxa have been reported from the Albian–Cenomanian-age Kem Kem beds of south-eastern Morocco. Lavocat (1955) briefly reported (without illustration) on fragments of a skull of a longirostrine form, which he named *Thoracosaurus cherifiensis*; this material, along with more complete specimens, has now been placed in a new genus *Elosuchus* by Lapparent de Broin (2002). Buffetaut (1976b) illustrated and referred a partial cranium to *Libycosuchus* sp.. Buffetaut (1994) designated a partial left dentary with six teeth (Musée des Dinosaures, Espéraza, no. MDE C001) as the holotype of *Hamadasuchus rebouli*, which he included in the family Trematochampsidae (see below). Subsequently, Larsson & Sidor (1999) referred isolated teeth from the Kem Kem beds to *H. rebouli* and other

*Corresponding author. E-mail: hans.ce.larsson@mcgill.ca

Downloaded from https://academic.oup.com/zoolinnean/article/149/4/533/2630922 by guest on 31 August 2021

multicuspid teeth to indeterminate crocodyliforms, and Prasad & Lapparent de Broin (2002) discussed the microstructure of teeth of *H. rebouli*.

In this paper, we describe a series of exquisitely preserved specimens that are referable to *H. rebouli* and are housed in the vertebrate palaeontological collections of the Royal Ontario Museum (ROM) in Toronto. They comprise the complete skull of a large individual (ROM 52620), the interorbital region of the skull roof of another larger specimen (ROM 54585), an associated snout and partial left mandibular ramus of a smaller individual (ROM 49282), posterior portions of two well-preserved crania (ROM 52059, with associated left jugal and quadratojugal, and ROM 54511), a fragmentary braincase (ROM 54113) of smaller specimens, a nearly complete right dentary of a large individual (ROM 52045), and a left dentary of a small specimen (ROM 52047). This wealth of superb new material permits, for the first time, a detailed account of the cranial structure of *H. rebouli* and an assessment of the phylogenetic position of this distinctive taxon within Crocodyliformes.

The fossils reported here were recovered by local collectors in south-eastern Morocco from predominantly red continental sandstones, which are known as the Kem Kem beds (Sereno *et al*., 1996). These strata are generally considered to be between Albian and Cenomanian in age because they are conformably overlain by limestones of late Cenomanian age (*Neolobites vibrayeanus* Zone; Courville *et al.*, 1991). The exact provenance for the fossils cannot be established. The Kem Kem beds have yielded abundant often exquisitely preserved, if typically disassociated, skeletal remains representing a diverse assemblage of fishes and reptiles (Russell, 1996; Sereno *et al*., 1996).

SYSTEMATIC PALAEONTOLOGY

CROCODYLIFORMES CLARK IN BENTON & CLARK (1988) MESOEUCROCODYLIA WHETSTONE & WHYBROW, 1983 *SENSU* CLARK IN BENTON & CLARK (1988) METASUCHIA BUFFETAUT, 1981 *SENSU* CLARK IN BENTON & CLARK (1988)

SEBECIA NOM. NOV. *HAMADASUCHUS REBOULI* BUFFETAUT, 1994

Referred specimens: ROM 52620, complete skull of a large individual (Figs 1–5); ROM 54585, interorbital region of the skull roof of another larger specimen; ROM 49282, associated snout and partial left mandibular ramus (Fig. 6) of a smaller individual; ROM 54512, fragmentary left maxilla of a smaller individual; ROM 52059, posterior portion a well-preserved braincase with the left jugal and quadratojugal (Fig. 7A–C); ROM 54511, posterior portion a well-preserved braincase (Fig. 7B–D); ROM 54513, fragmentary braincase of a smaller specimen; ROM 52045, nearly complete right dentary of a large individual; and ROM 52047, left dentary of a small specimen.

Revised diagnosis: differs from other known crocodyliforms in the following combination of characters in adult specimens. Contribution of nasals to internarial bar exceeding 50%; dorsomedial edges of supratemporal fenestrae level with skull table; tapered distal squamosal prong; large posteroventral process on postorbital that contacts quadrate and quadratojugal; external auditory meatus fossa extending anteriorly over entire length of postorbital; supratemporal fossa covering most of bony bar between supratemporal fenestra and orbit; thickened premaxillary extension over posterodorsal corner of external naris forming notch; small incisive foramen; palatine–pterygoid suture extending to posterior angle of suborbital fenestra; ectopterygoid–maxilla suture approaching posteromedial margin of maxillary tooth row; absence of posterior ectopterygoid process along ventral surface of jugal; absence of prominent crest on dorsal surface of distal end of quadrate; and prominent bilateral posterior projections on posterodorsal surface of supraoccipital. An autapomorphy not previously reported in other crocodyliforms is the presence of shallow dorsal and ventral grooves extending anteriorly from the antorbital fossa (the fossa is only present on one side in the single complete cranium currently known for *Hamadasuchus*).

Distribution: Kem Kem beds, south-eastern Morocco. Age: Cretaceous (Albian–Cenomanian).

DESCRIPTION

SKULL

The following anatomical description is based primarily on the superbly preserved skull ROM 52620 (Figs 1–5). The only preservational deficiencies of this specimen are either damage to or loss of several teeth, the loss of the palpebral bones (the former presence of which is indicated by articular facets on adjoining cranial elements), an oblique (repaired) fracture through the snout, some breakage in the palatal region, and minor damage to the braincase in the proximal region of the right paroccipital process. As a result of distortion during fossilization, the sides of the snout are no longer symmetrically aligned so that the rostrum appears skewed towards the right when viewed from the front.

In dorsal view, the outline of the cranium is that of an elongate triangle. (See Table 1 for selected measurements of ROM 52620.) Snout length in ROM 52620 is about 70% of the basal skull length – the

Downloaded from https://academic.oup.com/zoolinnean/article/149/4/533/2630922 by guest on 31 August 2021

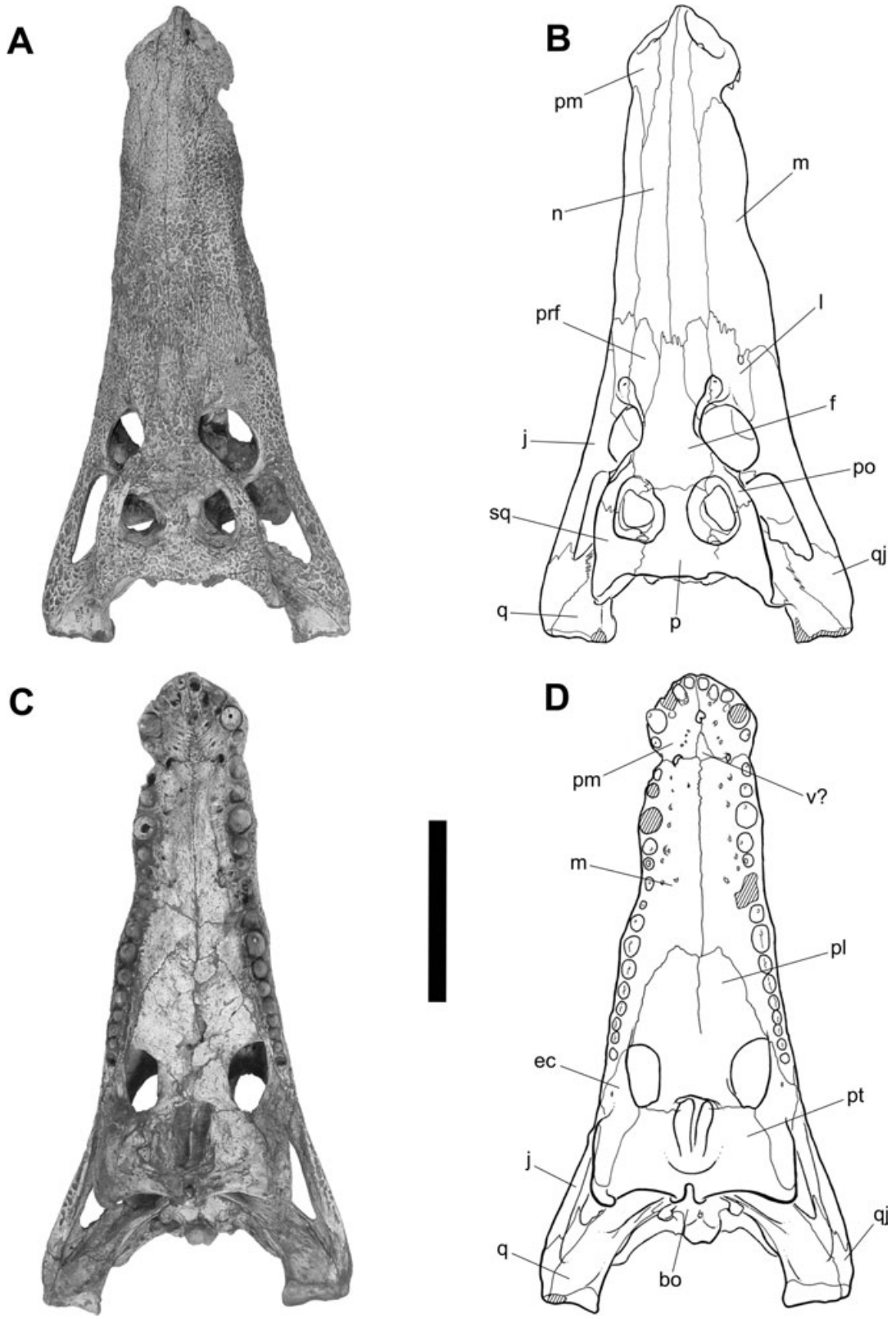

Figure 1. Cranium of *Hamadasuchus rebouli* (ROM 52620). A, dorsal and C, ventral view. B and D, outline drawings corresponding to each view. Scale bar = 10 cm. Anatomical abbreviations are defined in Appendix 1.

Downloaded from https://academic.oup.com/zoolinnean/article/149/4/533/2630922 by guest on 31 August 2021

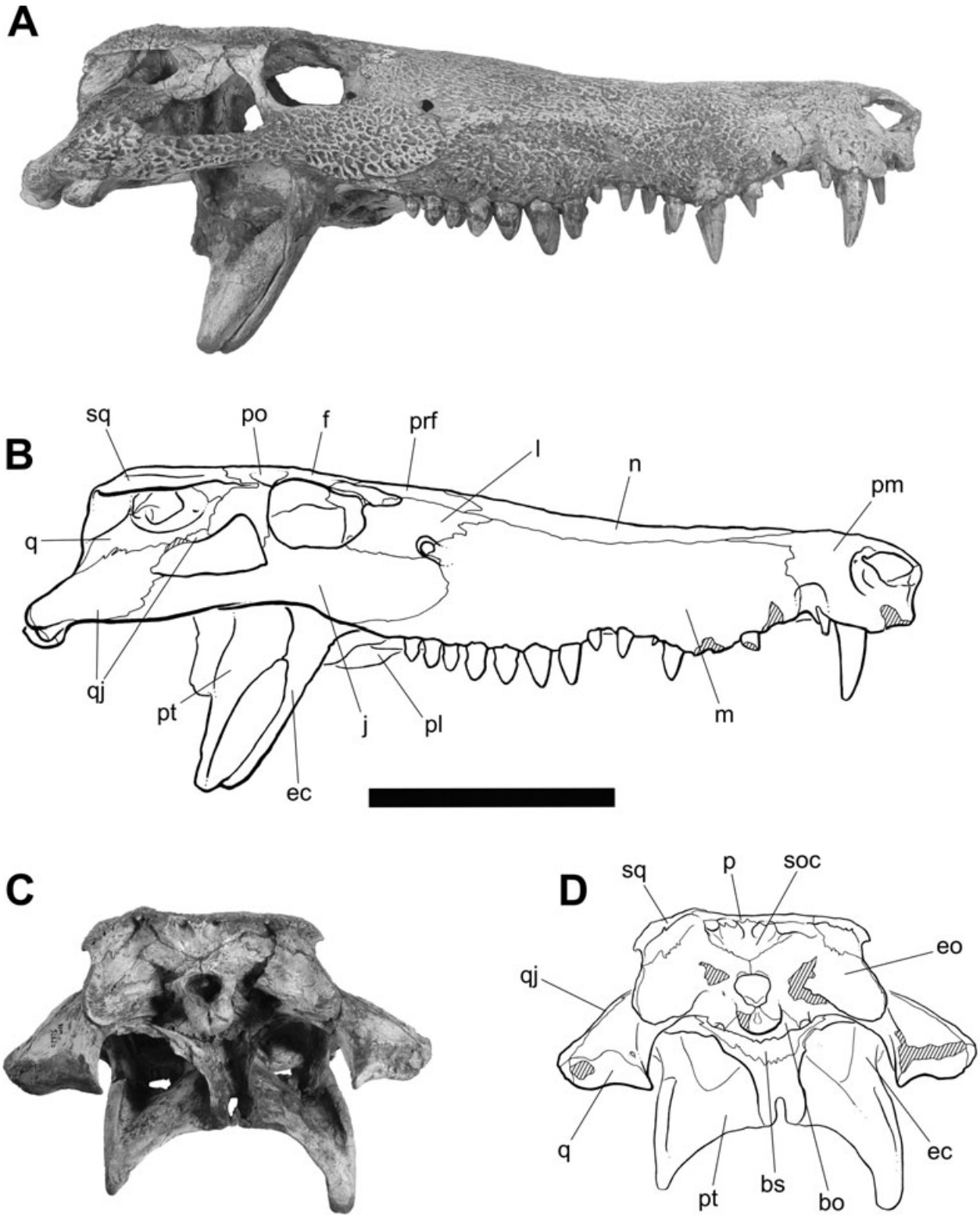

Figure 2. Cranium of *Hamadasuchus rebouli* (ROM 52620). A, right lateral and C, occipital view. B and D, outline drawings corresponding to each view. Scale bar = 10 cm. Anatomical abbreviations are defined in Appendix 1.

Downloaded from https://academic.oup.com/zoolinnean/article/149/4/533/2630922 by guest on 31 August 2021

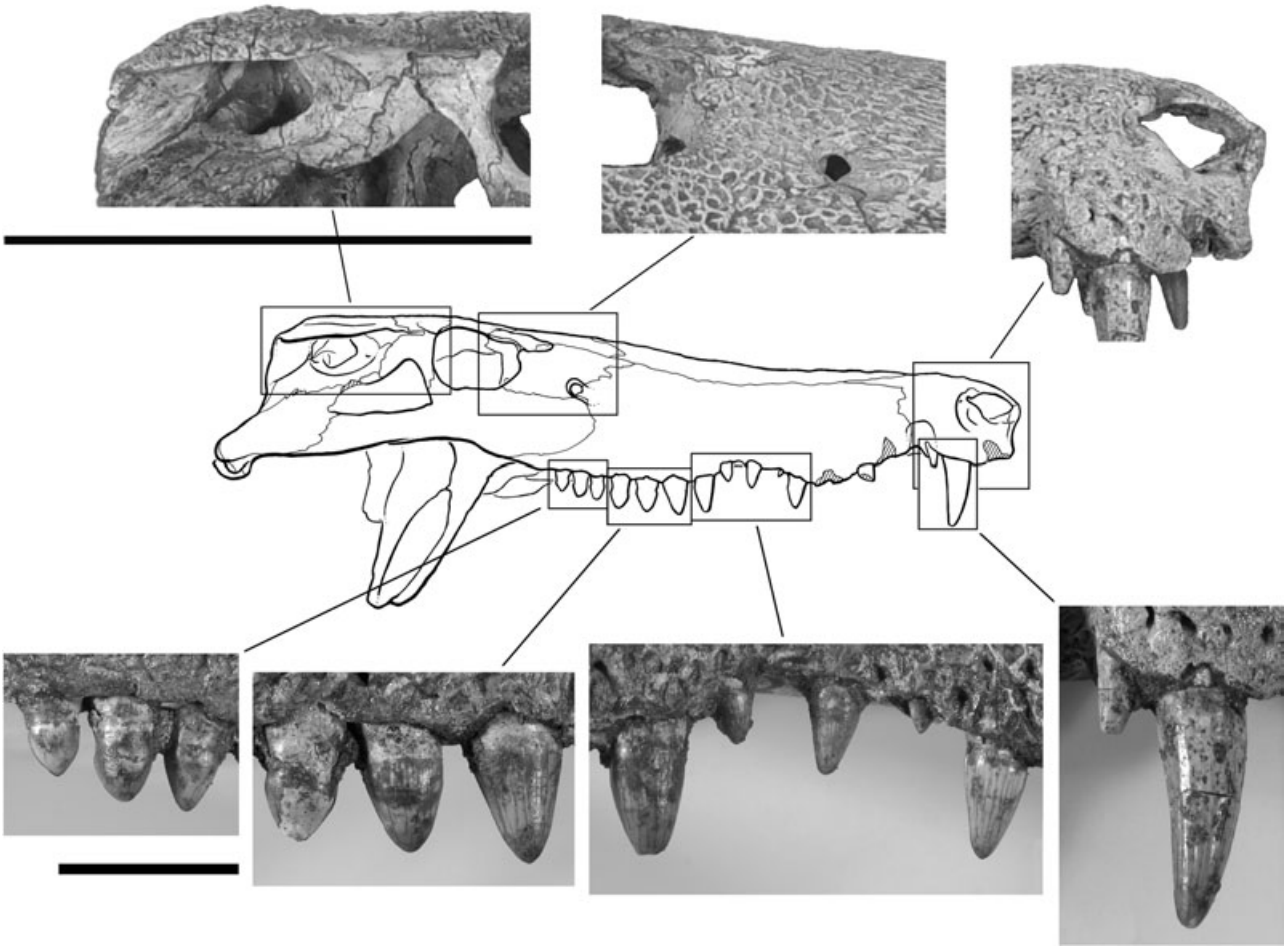

Figure 3. Details of the cranium of *Hamadasuchus rebouli* (ROM 52620). Upper details are to same scale; scale bar = 10 cm. Details of the dentition are to same scale; scale bar = 2 cm.

value used by Busbey (1995) to distinguish between 'normal' and 'long' snouts in crocodyliform reptiles. The rostral tip of the snout is slightly pointed in dorsal view. The sides of the snout are not sharply demarcated from the skull roof, and the skull table is continuous with the dorsal surface of the snout. The external surfaces of the dermal bones are distinctly sculptured with pits and ridges. This sculpturing is particularly pronounced on the jugal, quadratojugal, and skull table, and is least developed on the premaxilla. The paired external narial fenestrae face laterally, as well as somewhat anteriorly, and are separated by a robust bony bar. The antorbital fenestra, which is present only on the right side of the snout in ROM 52620, is small, circular, and only slightly recessed. The more or less circular orbit faces laterally and slightly anterodorsally. Judging from the articular facets along the dorsal margin of the opening, it was completely roofed by palpebrals. The supratemporal fenestra is smaller than the orbit and longer than wide, with its long axis extending in an anteroposterior direction. The lateral border of the supratemporal fenestra is nearly straight in dorsal view, whereas the medial margin is laterally concave. The subtriangular infratemporal fenestra is larger than either the orbit or the supratemporal fenestra. It faces dorsolaterally and slightly anteriorly. The suborbital (palatal) fenestra is of moderate size, and its long axis is orientated anteroposteriorly. The anterior end of this opening is located at the level of the space between maxillary teeth 14 and 15. The choanae occupy much of the anteromedial portion of the pterygoids and are bounded anteriorly by the palatines. The choanal opening is longer than wide and divided by a median bony septum formed by the pterygoids. It opens ventrally rather than posteroventrally as in many crocodylians.

The premaxilla forms most of the margin of the external naris and, together with its fellow, the

Downloaded from https://academic.oup.com/zoolinnean/article/149/4/533/2630922 by guest on 31 August 2021

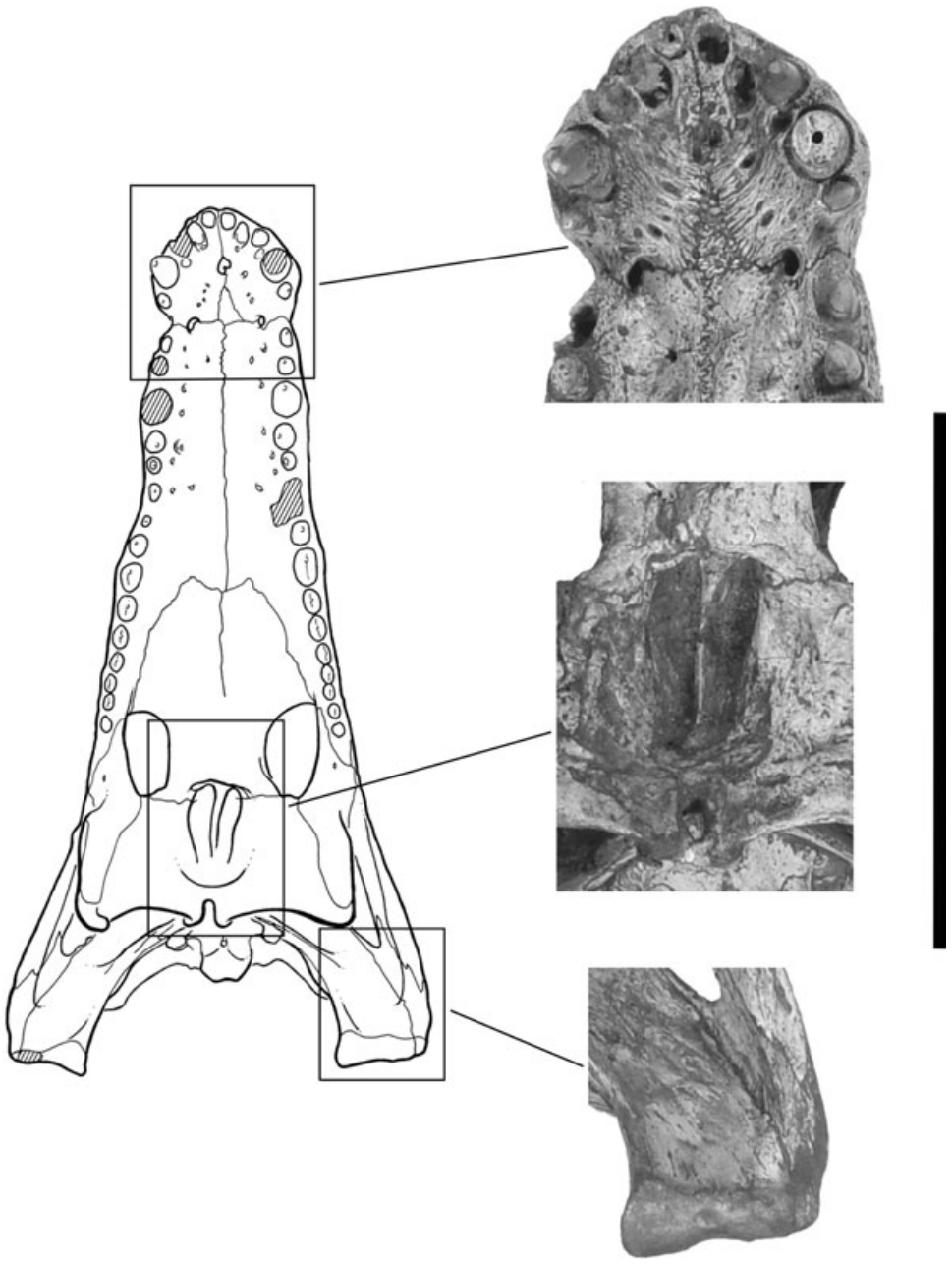

Figure 4. Details of the cranium of *Hamadasuchus rebouli* (ROM 52620). Scale bar = 10 cm.

anterior third of the internarial bar. The premaxillary contribution to the internarial bar meets the nasal portion of the bar at the anterior extent and mid-height of the labial process of the premaxilla. The process projects anteriorly slightly beyond the alveolar margin of the premaxillae. A pair of openings is located immediately posterior to the anterior base of the internarial bar. These features appear to be damaged regions of thin bone covering the pit that received the anterior dentary teeth in life. The anterior surface of the anterior process of the premaxilla is pitted with numerous tiny foramina. Anteriorly, its base is marked by several foramina near the alveolar margin. Several large foramina are situated along the periphery of a smooth, depressed area that surrounds the narial fenestra posterolaterally and ventrolaterally. A large foramen is situated in the posterolateral extent of this depression. The posterodorsal corner of the circumnarial depression is roofed to form a lateral recess by an anterior projection of the premaxilla, which extends forward along the posterior portion of the internarial bar for a short distance. Posteriorly, the

Downloaded from https://academic.oup.com/zoolinnean/article/149/4/533/2630922 by guest on 31 August 2021

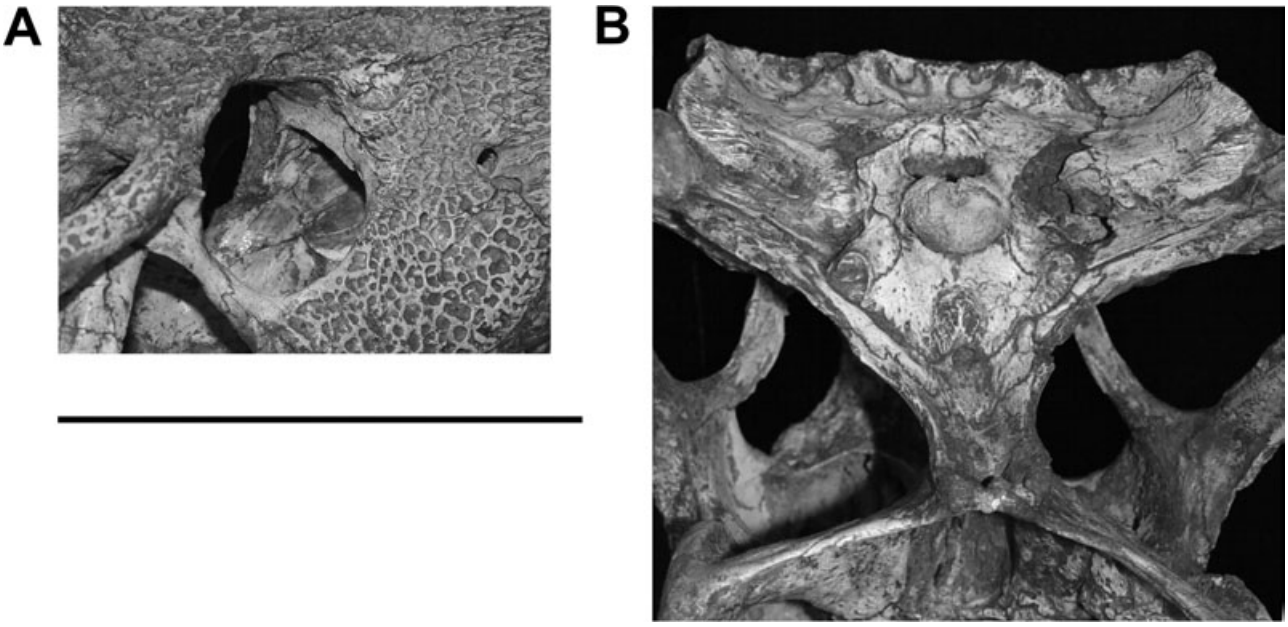

Figure 5. Details of the cranium of *Hamadasuchus rebouli* (ROM 52620). A, right posterodorsolateral view into orbit showing prefrontal pillar. B, posteroventral view of occiput. Scale bar = 10 cm.

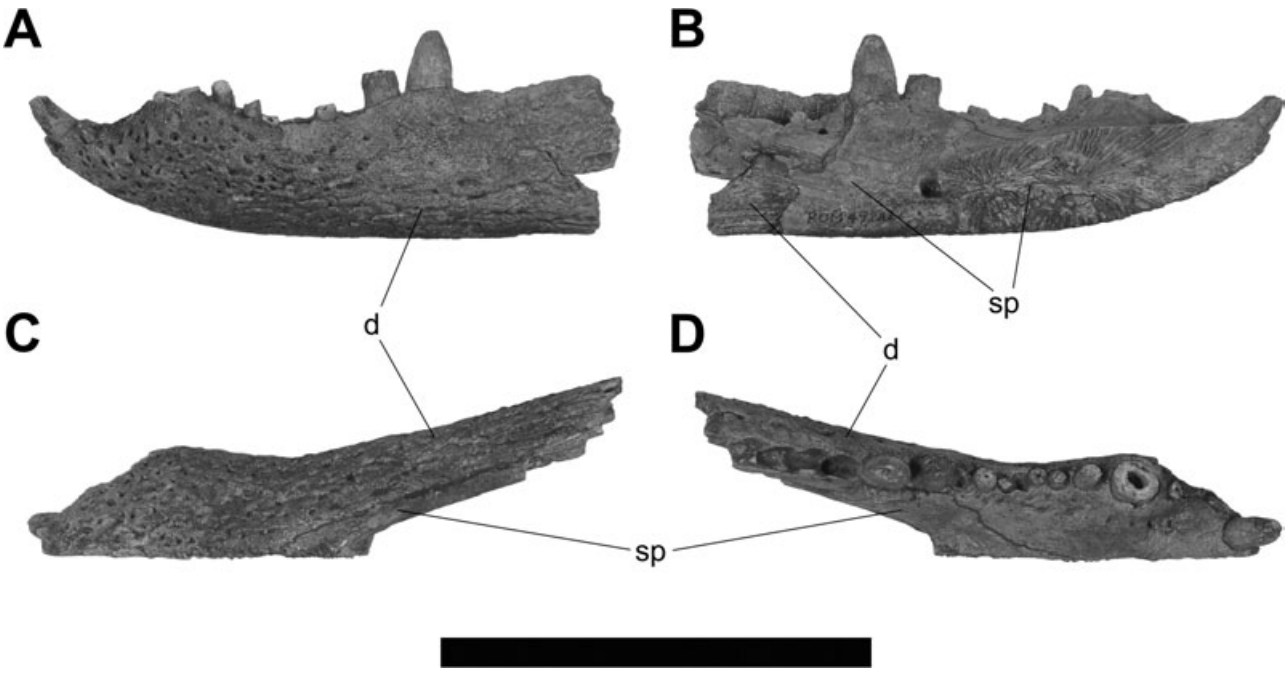

Figure 6. Partial left dentary of *Hamadasuchus rebouli* (ROM 49282) in A, lateral, B, medial, C, ventral, and D, dorsal views. Scale bar = 10 cm. Anatomical abbreviations are defined in Appendix 1.

premaxilla, together with the anterior portion of the maxilla, forms a conspicuous, laterally, and ventrally facing notch for the reception of the greatly enlarged fourth dentary tooth on either side of the snout (ROM 49282). This notch encroaches upon the alveolar margin of the fourth premaxillary tooth, exposing part of the tooth root within the notch, and forming a diastema between the premaxillary and maxillary teeth. In dorsal view, the two notches appear as a marked constriction between the premaxilla and

Downloaded from https://academic.oup.com/zoolinnean/article/149/4/533/2630922 by guest on 31 August 2021

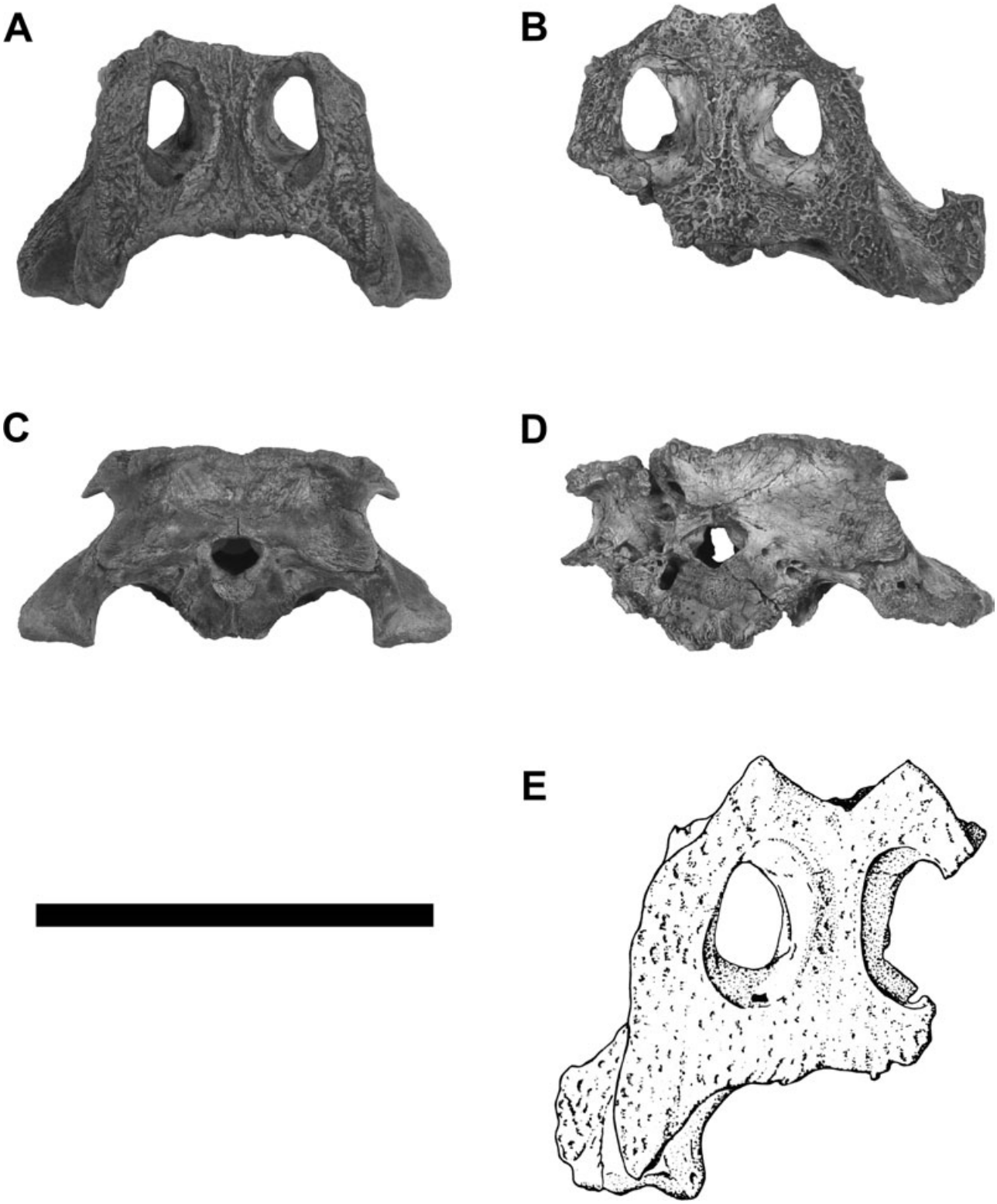

Figure 7. Partial juvenile crania of *Hamadasuchus rebouli*. A and C, dorsal and occipital views of ROM 52059. B and D, dorsal and occipital views of ROM 54511. E, partial cranium of Moroccan '*Libycosuchus*' (modified from Buffetaut, 1976: fig. 3). Scale bar = 10 cm.

Downloaded from https://academic.oup.com/zoolinnean/article/149/4/533/2630922 by guest on 31 August 2021

Table 1. Selected measurements (in cm) for the skull of *Hamadasuchus rebouli* (ROM 52620)

Basal skull length (from tip of snout to occipital condyle along midline)	32.5
Length of skull (from posterior end of skull table to tip of snout, on midline)	32.4
Length of snout (from anterior end of orbit to tip of snout)	22.8
Greatest transverse width of skull (across quadratojugals)	17.6
Least transverse interorbital distance	3.0
Transverse width of skull at level of anterior ends of orbits	10.9
Transverse width of skull at level of postorbital bars	12.2
Transverse width of skull table anteriorly	7.4
Transverse width of skull table posteriorly	9.9

maxilla. The large posterodorsal process of the premaxilla tapers posteriorly and is wedged between the maxilla and nasal, extending back to the level of the large third maxillary tooth. Laterally, the premaxilla contacts the maxilla along a nearly vertical suture within the notch. Each premaxilla holds four teeth. Maximum labiolingual diameters for premaxillary, maxillary, and dentary teeth are given in Table 2. The first and fourth premaxillary teeth are the smallest; the third is greatly enlarged and overhangs the dentary laterally (ROM 49282). A deep occlusal pit between, as well as lingual to, the first and second premaxillary alveoli received the tip of the procumbent first dentary tooth (ROM 49282). The palatal shelves of the premaxillae are transversely concave ventrally. They meet medially to form the anterior end of the secondary bony palate and enclose between them a small incisive foramen, which is located just behind the alveolar margin. The medial margins of these shelves are fringed by numerous finger-like extensions along their entire length. There are several possibly neurovascular openings of various sizes on the palatal aspect of the premaxillae. On either side of the snout, a large foramen, possibly for the passage of a palatal branch of ramus maxillaris of nervus trigeminus (V2), is located on the transverse suture between the premaxilla and maxilla, just medial to the palatal edge of the lateral notch.

The long, moderately deep maxillae comprise most of the sidewalls of the snout. Medially, the palatal shelves of the maxillae broadly meet to form an extensive secondary bony palate. The maxilla slopes steeply down from the region of the nasals. Its alveolar margin is distinctly festooned with two 'waves' (the anterior one of which is more pronounced), which reach their greatest depth at the third and ninth maxillary tooth, respectively. Each maxilla holds 16 closely spaced teeth. The tooth crowns have distinct, finely serrated anterior and posterior cutting edges (carinae). The third tooth is the largest in the maxillary tooth row, and the ninth is the second largest. The teeth posterior to the ninth are small but proportionately stouter, and show a distinct constriction between the crown and root. The crowns of these posterior teeth are less conical than those of the anterior ones and are D-shaped in transverse section, with an anteroposteriorly convex labial and a nearly flat lingual surface. They also lack the vertical fluting present on the premaxillary and anterior maxillary teeth, especially the larger ones. On all well-preserved tooth crowns, the enamel shows fine wrinkling. (No maxillary teeth are preserved in the smaller specimens in our study sample.) The maxillary tooth row ends posteriorly at the level of the anterior margin of the orbit, and the maxilla extends back only a short distance from that point, terminating just behind the anterior margin of the orbit. The tooth rows diverge slightly more posteriorly. Posterolaterally, the maxilla is bounded by the jugal and lacrimal. In ROM 52620, there is no antorbital fenestra on the left side of the snout, but a small (6-mm long), subcircular opening is present on the right side. The asymmetry neither results from preservation nor any obvious pathology. The fenestra is bounded dorsally and posteroventrally by the lacrimal, and anteriorly and ventrally by the maxilla. A narrow fossa surrounds the opening and continues onto the lateral aspect of the maxilla in the form of two shallow grooves, the broader ventral one of which also extends onto the lacrimal. Several foramina mark the palatal shelf of the maxilla just lingual to the tooth row. Two deep occlusal pits for the reception of the large dentary teeth 12 and 13 are situated immediately lingual to maxillary teeth 5–7 (ROM 49282). Similar occlusal pits are present, but less well defined, on ROM 52620. A wide groove extends forward from these pits on either side of the secondary bony palate to the foramen on the palatal suture between the premaxilla and maxilla. The disposition of these occlusal features indicates the presence of a complete overbite. Medially, the palatal shelves of the maxillae form a ventrally convex thickening or torus that is most pronounced anteriorly and merges into the palate posteriorly at the level of the eighth maxillary tooth. The anterior portion of this torus ascends to the sutural contact between the premaxilla and maxilla on the palate, whereas its posterior region graduates into the flat palatal shelves of the palatines. The suture between the maxilla and palatine on the palatal surface extends more or less transversely close to the midline, but then turns posterolaterally and continues back almost to the level of the fourteenth maxillary tooth. The maxilla barely enters into the lateral margin of the suborbital

Downloaded from https://academic.oup.com/zoolinnean/article/149/4/533/2630922 by guest on 31 August 2021

Table 2. Maximum labiolingual and mesiodistal diameters (in mm) of premaxillary (pm) and maxillary (m) alveoli (ROM 52620 and ROM 49282), and dentary alveoli (d) (ROM 49282 and ROM 52045) of *Hamadasuchus rebouli*. When possible, the average of the left and right corresponding tooth positions are given

Cranial tooth position	ROM 52620		ROM 49282	
	labiolingual	mesiodistal	labiolingual	mesiodistal
pm1	7.3	5.8	6.0	?
pm2	9.0	7.0	6.5	6.5
pm3	13.0	12.3	10.0	10.5
pm4	6.3	4.5	5.5	5.8
m1	6.5	8.0	6.0	7.0
m2	8.5	8.5	7.5	7.5
m3	13.0	13.5	11.0	13.0
m4	9.0	8.0	7.5	6.8
m5	7.5	7.0	6.0	7.0
m6	6.3	8.0	4.5 (3.5)†	6.3 (5.0)†
m7	5.5	6.0	6.0	7.5
m8	9.0	10.3	9.0	9.0
m9	10.5	13.3	8.8	10.5
m10	8.5	9.5	7.5	8.0
m11	8.0	8.5	7.0	7.8
m12	7.0	7.3	5.3	6.5
m13	6.0	6.5	4.5	5.5
m14	5.8	6.0		
m15	5.3	6.3		
m16	6.5*	6.5*		

Mandibular tooth position	ROM 52045		ROM 49282	
	labiolingual	mesiodistal	labiolingual	mesiodistal
d1	6.5	?	8.0	9.0
d2	4.0	4.5	5.0	5.5
d3	3.5	4.0	4.5	5.0
d4	11.5	12.0	9.5	11.5
d5	5.5	6.0	6.0	6.5
d6	4.5	2.5	4.5	4.5
d7	4.0	3.0	4.0	4.0
d8	3.0	3.5	4.0	4.0
d9	3.0	3.5	4.0	4.0
d10	4.0	4.0	5.0	5.5
d11	6.5	8.0	5.5	6.0
d12	9.0	9.5	7.0	7.5
d13	9.5	12.0	7.5	11.0
d14	8.0	9.5	5.0	7.0

*Present only on left side; †obvious extra alveolus between m6 and m7.

fenestra before being excluded by the palatine anteriorly and ectopterygoid posteriorly.

The jugal is long and transversely narrow. Its anterior (infraorbital) process forms a dorsoventrally deep lappet, which borders the orbit posteroventrally and has a nearly straight sutural contact with the lacrimal. On the right side of the snout in ROM 52620, the jugal is barely excluded from the ventral margin of the antorbital fenestra by a short process of the lacrimal. The orbital margin of the jugal is somewhat thickened laterally just anterior to the postorbital bar and has raised sculpturing. The margin is not laterally

Downloaded from https://academic.oup.com/zoolinnean/article/149/4/533/2630922 by guest on 31 August 2021

everted. The slender postorbital bar is situated at about mid-length, and is only slightly inset from the surface of the jugal body. The jugal overlaps the postorbital anterolaterally at about mid-height on the postorbital bar. The posterior (infratemporal) process is only half as deep as, but thicker transversely than, the anterior process and forms the ventral margin of the large infratemporal fenestra. It expands slightly dorsoventrally near its posterior end in ROM 52620. The dorsal margin of the posterior process forms a distinct longitudinal ridge. The same region in the smaller specimen ROM 52059 lacks a distinct ridge because of a relatively thicker posterior process that is elliptical in cross-section.

The long nasal extends from the internarial bar back to the frontal. It is wide and extends in a nearly horizontal plane. The nasals have nearly parallel sides but expand slightly posteriorly. Anteriorly, they meet the short internarial processes of the premaxillae and form most of the dorsal margins of the external nares. The nasals are almost flat in this region, but gradually become transversely convex more posteriorly. Posteriorly, they contact the frontals along a short, interdigitating, anteriorly facing and V-shaped suture. The nasal extends for a short distance lateral to the frontal and separates the anterior ends of the frontal and prefrontal. It also extends along the anterolateral edge of the prefrontal, separating it anteriorly from the lacrimal and establishing a sutural contact between the lacrimal and nasal. Laterally, each nasal forms a long, fairly straight suture with the posterodorsal process of the premaxilla, the maxilla, and the lacrimal.

The transversely narrow prefrontal forms the anteromedial margin as well as part of the anterior wall of the orbit. The anterior tip of the prefrontal extends beyond the anterior extent of the frontal. Laterally, the prefrontal has a long suture with the lacrimal. The superficial course of this suture passes into a deep fossa near the orbital margin. This fossa extends largely into the lacrimal but borders the prefrontal as well. The depression on the prefrontal continues along the orbital rim to the posterior limit of the prefrontal. This depression is presumably related to the presence of a large anterior palpebral (which is not preserved in any of the available specimens of *Hamadasuchus*, but is present in related crocodyliform taxa). A large vascular foramen is present in the anterodorsal portion of the medial wall of the orbit. Although the opening lies near the suture between the lacrimal and prefrontal, it is located entirely within the prefrontal and immediately under the anteromedial roof of the orbit. A foramen for the nasolacrimal duct is situated on the suture between the prefrontal and lacrimal at mid-height on the orbital wall. The prefrontal contributes to a nearly vertical orbital wall. This septum is nearly half the height of the orbit and forms the posterior boundary of a large, subspherical recess. This recess probably housed a pneumatic diverticulum that communicated with the narial passage (Witmer, 1997). A slender, somewhat anterodorsally inclined process of the prefrontal pillar descends to contact the pterygoid and palatine ventromedially. The base of the prefrontal pillar is expanded anteroposteriorly to contact the palatine and pterygoid equally along a faint suture.

The large lacrimal makes up much of the anterior margin and wall of the orbit. The edge of the large fossa formed by the lacrimal and prefrontal is confluent with the surface of the lacrimal along its anterior and lateral margins. The posterior edge, however, is slightly undercut but still sculptured. The sutural contact between the lacrimal and jugal differs slightly on either side of ROM 52620. On both sides, however, the jugal overlaps the lacrimal at the extreme anterior end of the suture, the lacrimal overlapping the jugal along the remainder of the anterior two thirds of the suture, and both bones are in contact along a flush, interdigitating suture along the posterior third.

The anterior half of the dorsal surface of the unpaired (in dorsal view) subtriangular frontal is nearly flat. This surface becomes slightly transversely concave from near the mid-length of the orbits to the frontoparietal contact. ROM 52059 and ROM 54511 each bear a low sagittal crest on the posterodorsal region of the frontal (Fig. 7A). A similar but more pronounced crest is present on ROM 52059, and terminates at the frontoparietal suture. The larger specimen ROM 52620 shows no sign of a sagittal crest. The most anterior part of the short orbital rim of the frontal is grooved for contact with a palpebral. The frontal is depressed posterolaterally where it participates in the anteromedial portion of the supratemporal fossa. The frontal does not enter into the margin of the supratemporal fenestra. Posteriorly, it meets the parietal along an almost transverse suture, which extends between the anterior ends of the supratemporal fossae. Posteroventrally, the frontal is broadly contacted by the expanded proximal ends of the laterosphenoids, which leave only a narrow median passage for the olfactory and optic tracts. The laterosphenoid contacts the frontal along an arcuate, anteromedially extending groove that extends to the low cristae cranii on the ventral surface of the frontal.

The unpaired parietal forms the medial margins of the supratemporal fenestrae and fossae. Anteriorly, the parietal contacts the postorbital within the supratemporal fenestra beneath the frontal. In ROM 52059 and ROM 54511, the medial margins of the fossae are marked by distinct rims, but this is not the case in ROM 52620, the largest available specimen. The medial margins of the supratemporal fenestrae extend relatively parallel to each other in ROM 54511 as a result of the presence of a discrete

Downloaded from https://academic.oup.com/zoolinnean/article/149/4/533/2630922 by guest on 31 August 2021

fossa at the junction between the frontal, parietal, and postorbital. This fossa is absent in ROM 52059 and ROM 52060, both of which have laterally concave supratemporal margins. The medial surfaces of the supratemporal fenestrae face dorsolaterally and are smooth with no evidence of foramina. The posteromedial surface of the parietal is slightly different in the three specimens that preserve this region. The parietal of ROM 52059, the smallest specimen, bears a pair of low and rounded parasagittal crests that extend from the mid-length of the supratemporal fenestrae to near the posterior margin of the parietal. The element in ROM 54511, a medium-sized specimen, has a posteriorly facing V-shaped depression. The parietal of ROM 52620, the largest specimen, has a nearly flat surface pitted with wide but shallow sculpturing. The posterior margin of the parietal is slightly concave transversely. Posterolaterally, the parietal contacts the squamosal on the dorsal surface of the skull table at about the midpoint of the posterior margin of the supratemporal fenestra. A transversely oval post-temporal foramen (for the passage of arteria temporo-orbitalis) is located on the nearly vertical posterior wall of the supratemporal fossa on the suture between these two bones. The parietal forms the dorsal margin of the foramen, and the remainder is bounded by the squamosal. The transverse suture between the parietal and supraoccipital extends just below the posterior edge of the skull table and is concealed from dorsal view.

The postorbital comprises the anterolateral corner of the skull table and forms a dorsally sculptured bar separating the orbit from the supratemporal fossa. It forms the posterolateral margin of the orbit dorsally as well as the anterolateral margin of the supratemporal fenestra and fossa. In ROM 52620, the anterolateral corner of the postorbital bears a rugose depression along the orbital margin, which probably was for contact with a posterior palpebral. The depression contributes to the blunted corner of the postorbital that exhibits an anteromedially directed edge rather than a 90° corner found in many other crocodyliforms. The anterior extension of the auditory fossa lies on the lateral surface of the postorbital. A dorsolateral shelf formed by the postorbital anteriorly and the squamosal posteriorly overhangs the body of the postorbital. The fossa extends up to the anterolateral edge of the postorbital bar. The anterodorsolateral end of the postorbital terminates in a short spur that projects into the orbit. This spur would have underlain the posterior palpebral. The slender postorbital bar is transversely oval in cross-section. A large posteroventral process extends from the body of the postorbital at the apex of the infratemporal fenestra. This process contacts the squamosal dorsally, the quadrate along its posterodorsal margin, and the quadratojugal distally in an anteriorly facing slot on that bone.

The squamosal comprises the posterolateral corner of the skull table. It is slightly transversely concave dorsally with a distinctly sculptured dorsal surface. The lateral edge of the squamosal is nearly straight in dorsal view and bears a narrow longitudinal sulcus, which presumably served for the attachment of muscles associated with an external ear flap (as in extant crocodylians; Shute & Bellairs, 1955). The dorsal and ventral edges of this groove are on the same vertical plane. Anteriorly, the squamosal is overlapped by the postorbital at about mid-length of the supratemporal fossa, but continues anterolaterally to near the apex of the infratemporal fenestra. Ventrally, it broadly contacts the quadrate in front of and behind the otic foramen. Posteriorly, the squamosal forms a flange that extends posterolaterally from the skull roof. The flange is nearly confluent with the skull roof in ROM 52620, dorsally sculptured except for its posterolateral edge, and tapered distally. The flange in ROM 54511 is slightly deflected posterolaterally from the skull roof, but has sculpture similar to that in ROM 52620. The flange in ROM 52059 is entirely unsculptured, deflected ventrally from the skull table, and terminates as a broad lappet. The posteroventral process of the squamosal forms a nearly vertical plate, which extends posterolaterally, parallel to the paroccipital process. The anterolateral surface of this lobe-like structure marks the course of the external auditory meatus and is overhung by the lateral margin of the dorsal portion of the squamosal, which curls over the otic recess and the meatus. This configuration creates a posteriorly opening auditory meatus that is visible in occipital view. A shallow, ventral concavity is present on the squamosal over the otic recess. The squamosal has only a narrow exposure on the dorsolateral corner of the occiput. In posterior view, the suture between the squamosal and paroccipital process is interdigitated along its medial half and straight distally.

The quadratojugal forms much of the posterodorsal margin of the infratemporal fenestra. Except for its anterodorsal portion, the lateral surface of the quadratojugal is heavily sculptured. The narrow anterodorsal ramus has a long sutural contact with the quadrate, which becomes distinctly interdigitated anteriorly. The ramus contacts the postorbital to exclude the quadrate from the margin of the infratemporal fenestra. The infratemporal margin of the quadratojugal is smooth and lacks a spina quadratojugalis. A slight curve is present in the margin at the quadratojugal–postorbital contact and may indicate the attachment for musculus levator bulbi, which attaches to the spina in extant crocodylians with this feature. The posterior corner of the infratemporal

Downloaded from https://academic.oup.com/zoolinnean/article/149/4/533/2630922 by guest on 31 August 2021

fenestra is formed by the quadratojugal. A short process of the quadratojugal extends anteriorly along the medial surface of the infratemporal process of the jugal for about one third of the length of the infratemporal bar. The posteroventral portion of the quadratojugal forms a lateral extension to the mandibular condyle. A distinct constriction separates the condylar region of the quadratojugal from the remainder of that element. This extension places the quadratojugal within the jaw joint; its rounded posterior end is continuous with the distal articular surface of the quadrate.

The large quadrate forms most of the jaw joint and is sutured to the lateral wall of the braincase. It is anterodorsally inclined so that its distal articular surface is situated posterior and ventral to the occipital condyle in typically crocodyliform fashion. The approximately transverse articular surface faces posteroventrally and is slightly constricted in the middle, dividing it into two ventromedially orientated condyles. A dorsal extension of this surface is developed over the medial condyle. The extension is associated with a crest that extends from the condyle to the contact between the quadrate and paroccipital process in ROM 52059 and 54511. This crest is absent in ROM 52620, which has a low, broad ridge in its place. A foramen aërum (for the posterior exit of the siphonium) is situated on the posterodorsal surface of the quadrate near the dorsomedial margin of the medial condyle. The foramen opens into a small fossa that borders the articular edge of the condyle. The large otic foramen is more or less oval in outline with an acute dorsal apex formed between the squamosal and primary head of the quadrate. The posterodorsal margin of the foramen is bounded by the squamosal and the posteroventral margin by the quadrate. A narrow groove separates the two bones at this margin and continues to the edge of the tympanic cavity. Lateral to the cavity, the groove is replaced by a straight suture. Anterior to the otic foramen, but still located within the tympanic cavity, an opening marks the anterior entry of the siphonium. Ventral to the latter foramen, a fossa ends in a blind pit on the anteroventral margin of the tympanic cavity. Although no other external pneumatic foramina are present, the proximal two thirds of the quadrate was hollowed by a complex set of pneumatic diverticula, evidenced by the fragmentary quadrates of ROM 54511 and ROM 54513. Ventromedially, the quadrate extends along the anteroventral edge of the paroccipital process to contact the basisphenoid anterolaterally. Anteriorly, against the braincase, it forms much of the margin of the large foramen for nervus trigeminus (V). The ventral margin of the quadrate is overlapped by the quadrate ramus of the pterygoid. Dorsomedially, the quadrate extends into the supratemporal fossa, contacting the ventral edge of the parietal and squamosal along a more or less horizontal suture that circumscribes the anterior surface of the fossa. The quadrate broadly contacts the laterosphenoid anteriorly along a nearly vertical suture. 'Crest B' (Iordansky, 1964, 1973) is the only sharply defined muscular crest on the ventral surface of the quadrate in ROM 52620. However, the quadrates of the smaller specimens ROM 52059 and ROM 54511 bear a second distinct crest, which extends medial and parallel to the ventral suture between the quadratojugal and quadrate; this feature, which probably corresponds to 'crest A' (Iordansky, 1964, 1973) in extant crocodylians, is represented by a muscle scar in ROM 52620. These features can be related to the development of musculus adductor mandibulae posterior (Iordansky, 1964, 1973).

A possible vomer appears to be present within the palatal suture between the premaxilla and maxilla. The bone is exposed as a triangular feature on the palate with its apex extending between the posterior premaxillary palatal shelves to the posterior margin of the incisive foramen. The palatal surface of the bone in ROM 52620 is covered with small rugose peaks that obliterate any sutures. However, the same region in the smaller specimen ROM 49282 is smoother and has a complex, layered suture that extends across the bone. This suture indicates that the bone is paired and overlaps its counterpart. The complex overlapping of these bones may indicate that they are, in part, anterior extensions of the maxillae.

The palatal shelves of the palatines form nearly the posterior half of the secondary bony palate along their entire length. The medial palatal contact with the maxillae forms a transverse suture in ROM 49282 but a slightly posteriorly pointed 'V' in ROM 52620. This suture traverses about one quarter of the palatal surface on either side before turning posterolaterally to extend towards the posterior maxillary teeth. The suture does not enter the maxillary tooth row and terminates at the level of the penultimate tooth and the anterolateral corner of the suborbital fenestra. The midline suture is relatively straight in its anterior half but becomes sigmoid more posteriorly in ROM 52620. The sigmoid shape may be caused by a possibly pathological condition in the midline of the palate in this region. The palatines extend partly into the margin of the choanae. The anterior margin is bounded by the pterygoids (described below), whereas the palatines form the anterolateral corners of the choanae. The palatal contact between the palatine and pterygoid extends transversely from inside the choanae to the suborbital fenestra. The palatines appear 'inflated' in the region of the suborbital fenestra. This pneumatic expansion is evident dorsally where the palatines enclose a chamber, but not ventrally as the chamber does not expand into the suborbital fenestra.

Downloaded from https://academic.oup.com/zoolinnean/article/149/4/533/2630922 by guest on 31 August 2021

Dorsomedially, the palatines form a tall median septum that extends anteriorly from the prefrontal pillars. An arcuate crest is located ventrolateral to the median septum and may have supported a pneumatic diverticulum of the narial passage.

Posteriorly, the pterygoids are fused to each other and form large, posteroventrally projecting flanges, which are linked by a broad, transversely concave and posteroventrally inclined sheet of bone. The lateral margins of the flanges are anteroposteriorly expanded and have a pitted surface that would have been covered by a cartilaginous cap in life. The sheet is thin and even pierced by a small foramen on the right side. It is smooth dorsally but pitted with numerous small depressions and grooves on its palatal surface. Anterior to this sheet, a wide depression on the palatal surface houses the choanal opening medially. The choanae open into a posteroventrally orientated depression on the pterygoid and are sagittally divided by a long pterygoid septum. The septum is recessed from the rim of the choanal opening and forms the anterior margin of the choanae slightly above the palatines. Behind that opening, posterior processes of the pterygoids extend posteroventrally. These processes bound the lateral margins of a tall notch. Posteriorly, the notch is confluent with the anterior face of the median eustachian fossa. This fossa is situated on a tall, vertical, and posteriorly concave sheet of bone. The dorsal half of this sheet is formed by the basisphenoid, whereas the pterygoids form the ventral half of this vertical sheet and taper dorsolaterally, continuing 'crest B' (Iordansky, 1964, 1973). The contact between the pterygoid and quadrate extends anteriorly along the braincase in a zigzag course that passes anteroventrally and then turns anterodorsally. At this apex, there is a shallow triangular depression on the quadrate. The pterygoid extends up to the contact between the laterosphenoid and quadrate below the trigeminal foramen. From this point on, the contact between the pterygoid and laterosphenoid extends anteriorly to the contact between the pterygoids, which form an anterior wedge. The wedge continues anteriorly to the prefrontal pillar, forming a sagittal crest in the interorbital space.

The ectopterygoid caps the anterolateral edge of the pterygoid flange, descending to a point just short of the distal end of the flange. The body of the ectopterygoid has an elongate elliptical outline in transverse section with its long axis directed somewhat anteromedially. Laterally, the ectopterygoid braces the jugal and contacts the ventral base of the postorbital bar. A foramen pierces the ventral surface of the ectopterygoid where it turns laterally to abut the jugal. The anterior process of the ectopterygoid passes over the medial surface of the jugal and maxilla. The dorsal edge of the process is horizontal along the jugal and turns anteroventrally along the maxilla to the palatal surface. Ventrally, the ectopterygoid meets the posterior end of the maxilla and covers the medial margin up to the level of the second last tooth. The suture between the ectopterygoid and maxilla extends parallel to the tooth row and is offset medially by only 1–2 mm. The ectopterygoid forms almost the entire lateral margin of the suborbital fenestra, but does not contact the palatine. Posteriorly, the ectopterygoid does not extend beyond the level of the postorbital bar, but does have a small, low-angled corner that may represent the elongate prong found in many other crocodyliforms.

The supraoccipital is confined to the occipital surface of the cranium. In occipital view, it is much wider than tall and bears a low median ridge, which is flanked on either side by a depression that probably served for insertion of the ligamentum nuchae. Its ventral edge is broadly angled, rather than sharply triangular as in extant crocodylians. A slit-like vacuity at the junction of the supraoccipital, squamosal, and otoccipital, just below the posterior edge of the skull table, represents a reduced post-temporal fenestra. The dorsolateral ends of the supraoccipital are thickened to form stout postoccipital processes, which terminate just ventral to the post-temporal fenestrae and probably served as the point of insertion for musculus transversospinalis capitis (Frey, 1988). The best-preserved left process extends approximately 6 mm from the occipital plane. Ventrally, the supraoccipital is excluded from the dorsal margin of the transversely ovoid foramen magnum by the median contact between the otoccipitals, which form a bony shelf over that opening. The mastoid antrum is exposed in ROM 54511 and extends through the supraoccipital with a number of blind diverticula extending into dorsal and ventral portions of this bone.

Anterodorsally, the laterosphenoid forms a distinctly capitate process. This process is expanded transversely and orientated in an anteromedial direction with its posterolateral part forming a condyle that abuts the postorbital. The anteromedial extension of the process traverses onto the frontal. Posterior to the postorbital, the laterosphenoid contacts the parietal dorsally along a horizontal suture within the supratemporal space to a level dorsal to the foramen for passage of nervus trigeminus (V). At this point, the laterosphenoid has a posterior contact with quadrate along an interdigitating suture that extends to the dorsal margin of the trigeminal foramen. The laterosphenoid forms the anterior as well as much of the dorsal and ventral margins of the trigeminal foramen. Its lateral surface bears an anterodorsally extending groove in ROM 54511. Ventral to this groove, the laterosphenoid has a distally expanded process. This process encloses a canal through which ramus oph-

Downloaded from https://academic.oup.com/zoolinnean/article/149/4/533/2630922 by guest on 31 August 2021

thalmicus (V1) and a branch of ramus mandibularis of nervus trigeminus (V3) probably passed anteriorly to supply musculus levator bulbi, as in many extant crocodylians (Iordansky, 1973). A small foramen on the anterior aspect of the laterosphenoid, lateral and slightly ventral to the median passage for the olfactory and optic tracts, marks the passage for nervus trochlearis (IV).

The prootic is not exposed on the lateral surface of the braincase, but is covered by the quadrate posteriorly and the laterosphenoid anteriorly. Within the trigeminal recess, the prootic forms the posterior as well as the posterodorsal and posterovental margins of the large foramen for the exit of nervus trigeminus (V). Together with the otoccipital, it forms a small tympanic bulla enclosing the inner ear medially.

As in other crocodyliforms, the exoccipital and opisthotic are indistinguishably fused into a single element (otoccipital). The otoccipitals meet medially and form a bony shelf roofing the foramen magnum, as well as all but the ventromedial margin of this opening. Each element forms a broadly concave posterior surface on the occiput and half of the dorsal margin of the foramen magnum. It also contributes the dorsolateral corner of the occipital condyle, most of which is made up by the basioccipital. Lateral to the foramen, two small, laterally facing foramina represented exits for branches of nervus hypoglossus (XII). Situated in a shallow, subtriangular depression with, and lateral to, the more lateral of the two hypoglossal openings, a larger, undivided, and ventrally facing foramen vagi served as the exit for nervi glossopharyngeus and vagus (IX–X), and, ventral and slightly medial to it, there is the posterior carotid foramen (for the entry of arteria carotis interna into the braincase), which opens posteroventrolaterally. Cranial nerves IX and X presumably left the cranial cavity through a narrow metotic fissure posteroventral to the tympanic bulla, as in extant crocodylians (Iordansky, 1973). The otoccipital forms a stout ventral process that terminates ventrolaterally in a tuberosity that is confluent with a smaller basioccipital rugosity. In extant crocodylians, musculus longus colli (including musculus rectus capitis) inserts on the tuber and median crest of the basioccipital (Frey, 1988), and may have also inserted on the hypertrophied ventral process of the otoccipital as well. Posteriorly, the cranioquadrate passage (for the principal ramus of nervus facialis (VII), arteria orbitotemporalis, and vena capitis lateralis; Iordansky, 1973) is enclosed between the distal portion of the posterolaterally curving paroccipital process of the otoccipital and the quadrate (ROM 54511). The posterior surface of the flattened distal end of the paroccipital process bears distinct striations along its lateral margin and twists somewhat posterodorsally along its longitudinal plane to conform to the posteriorly opening auditory meatus described above.

The basioccipital forms most of the occipital condyle. Its posterior surface is inclined so that it faces posteroventrally. The posterior articular surface of the condyle is marked by a shallow, dorsoventral median sulcus extending from a somewhat deeper notochordal pit. The condylar neck curves posteroventrally. Situated ventral to the condyle on the condylar neck, a small median foramen probably served for passage of arteria occipitalis. The posteroventral surface of basioccipital slopes anteroventrally at an angle of approximately 4° from the skull roof plane. This angle is similar to that of other crocodyliforms with verticalized braincases, such as *Crocodylus* and *Alligator*. A short but prominent median crest extends from this opening to the foramen intertympanicum (for the median eustachian tube) situated within a deep depression on the suture between the basioccipital and basisphenoid. At the edge of the intertympanic foramen, the crest bifurcates to wrap about the posterior edge of the foramen. The dorsal surface of the basioccipital forms the smooth, transversely concave floor of the cranial cavity. The midline of this surface is slightly pinched to form a discrete groove. Laterally, the basioccipital is concealed by the basisphenoid and pterygoid. In ROM 54511, a narrow opening is present on either side just in front of the otoccipital–basioccipital tuber between the basioccipital and (partially preserved) basisphenoid. These foramina probably served for the passage of the lateral eustachian tubes. A large rhomboid sinus is apparent in ROM 54511 where the lateral eustachian tube met the posterolateral branch of the median eustachian passage.

The basisphenoid is only exposed on the occipital surface of the cranium. The bone is visible ventrally only along the cleft that is bounded by the pterygoids and basioccipital. This condition represents the verticalized braincase that occurs in many other neosuchian, peirosaurid, and sebecid crocodyliforms. Its median portion has a deeply concave posterior surface ventral to the foramen intertympanicum. On either side, a narrow process extends dorsolaterally between the basioccipital and pterygoid. There is no suturally distinct parasphenoid, and the basisphenoid and parasphenoid appear to be indistinguishably fused (parabasisphenoid). The dorsoventrally deep anterior portion of the parabasisphenoid appears to be confluent with the pterygoids. The dorsum sellae of the sella turcica is perforated by three foramina, the large, paired anterior carotid foramina above a smaller foramen that probably served for passage of the ramus palatinus of nervus facialis (VII). The trapezoidal dorsal surface of the parabasisphenoid continues the smooth, transversely concave floor of the cavum cranii. The floor is pierced anteriorly by a pair of foramina

Downloaded from https://academic.oup.com/zoolinnean/article/149/4/533/2630922 by guest on 31 August 2021

for nervus abducens (VI). The entrances of these nerves into the sella turcica are not visible.

MANDIBLE

The partial left mandibular ramus of ROM 49282 comprises much of the dentary and the anterior portion of the splenial (Fig. 7). The dentary has 18 tooth positions, with either partial or complete tooth crowns preserved in alveoli 1–3, 5, 6, and 12–13; the total tooth count is uncertain because the dentary is incomplete at its posterior end. The tooth row of the nearly complete right dentary ROM 52047 has 17 alveoli, only the thirteenth of which still contains a tooth. The mandibular symphysis extends back to the level of the posterior margin of the eleventh alveolus in ROM 49282. In dorsal view, the splenial makes up nearly half of the symphysis along the midline (equivalent to seven tooth positions). In dorsal view, the suture between the dentary and splenial is narrowly tapered along the anterior half of the symphysis and angled posterolaterally along the posterior half. At the level of the back of the symphysis, the splenial borders the tooth row. In ventral view, the splenial only contributes to one fifth of the length of the symphysis (equivalent to four tooth positions). The ventral suture between the dentary and splenial parallels the medial edge of the mandible and is inset by approximately 5 mm from the edge. In medial view, the suture between the dentary and splenial is interdigitating and angled posteroventrally. Immediately behind the posterior end of the symphyseal facet, the splenial has a large, oval foramen that is probably homologous to the foramen intramandibularis oralis in extant crocodylians, where it transmits branches of ramus mandibularis of nervus trigeminus (V3) to the oral mucosa (Iordansky, 1973). The medial surface of the dentary concealed under the splenial of ROM 52047 indicates that some portion of these nerve branches, and perhaps arteria mandibularis, passed under the splenial to enter the symphysis through a foramen on the anterior edge of the suture between the dentary and splenial. The lateral surface of the dentary is distinctly sculptured with numerous deep pits in the symphyseal region, which grade into irregular grooves posteroventrally. In addition, a row of neurovascular foramina extends ventral and more or less parallel to the alveolar margin of the bone. The alveolar margin is distinctly festooned, with two 'waves' complementing the festooning on the maxilla (ROM 49282). The more pronounced anterior 'wave' reaches its greatest depth at the fourth dentary tooth. This tooth is the largest in and is raised above the level of the remainder of the tooth row, and the dentary bulges laterally at this tooth position. In ROM 49282, the large third premaxillary tooth occludes in a slight notch on the lateral surface of the dentary anterior to this bulge. The posterior 'wave' reaches its greatest depth at the thirteenth tooth. The large first and smaller second teeth are procumbent with the first occluding into a deep fossa described on the palatal shelves of the premaxilla. Six small, closely spaced teeth follow the greatly enlarged fourth tooth. Numerous vascular foramina are present on the dentary just lingual to the more anterior teeth. Starting at the eleventh tooth, the dentary teeth increase again in size, with the thirteenth being the largest of this series. The anterior ten tooth crowns are nearly conical, but, from the eleventh tooth back, the crowns become triangular in labial view and more flattened labiolingually. Most posterior teeth are missing in the specimens described here. Several dentary teeth in ROM 49282 show vertical fluting on both sides of the crown. On ROM 52045 and 52047, the more posterior teeth have finely serrated anterior and posterior carinae. There is apparently no dorsal exposure of the dentary lingual to the teeth behind the eleventh tooth. The lingual surface of the dentary bears the Meckelian canal, which was largely covered by the splenial in life. Ventrally, the dentary turns sharply lingually, forming a nearly horizontal ventral surface of the mandible, to meet the splenial.

PHYLOGENETIC RELATIONSHIPS OF *HAMADASUCHUS REBOULI*

Buffetaut (1994) referred *H. rebouli* to the family level taxon Trematochampsidae. He first proposed that family for the reception of *T. taqueti* (Buffetaut, 1974, 1976a), and subsequently assigned to it various primarily Gondwanan crocodyliforms that are characterized primarily by the shared possession of labiolingually flattened (ziphodont) teeth, a highly differentiated dentary tooth row, and a jaw joint incorporating the quadratojugal and surangular (e.g. Buffetaut, 1991, 1994). However, most 'trematochampsids' are known only from fragmentary material, including the nominal taxon *T. taqueti*, which is based on scattered skeletal remains of numerous individuals from the lower Upper Cretaceous ('Senonian') of Niger (Buffetaut, 1974, 1976a; see Discussion below). Other authors have either questioned or even rejected the monophyly of Trematochampsidae (Gasparini, Chiappe & Fernandez, 1991; Ortega, Buscalioni & Gasparini, 1996; Buckley & Brochu, 1999). Buffetaut (1991) referred certain crocodyliform taxa from the Cretaceous of South America, such as *Peirosaurus torminni* Price, 1955 from the Baurú Formation (Maastrichtian) of Brazil, to the Trematochampsidae, but Gasparini (1982) and Gasparini *et al*. (1991) reassigned these forms to a separate family Peirosauridae.

Downloaded from https://academic.oup.com/zoolinnean/article/149/4/533/2630922 by guest on 31 August 2021

A phylogenetic analysis was performed to examine how the addition of data from the more complete material of *H. rebouli* influenced the reconstruction of the phylogenetic relationships of fossil crocodyliforms. A matrix consisting of 33 taxa and 158 qualitative and parsimony informative characters was compiled (Appendices 2 and 3). A taxon labelled as juvenile *Hamadasuchus* was used to submit the suite of presumed juvenile specimens of *Hamadasuchus* to phylogenetic scrutiny. Two taxa, *Orthosuchus stormbergi* and *Hsisosuchus*, were used as outgroups, and the other 25 taxa were collectively designated as the ingroup. Data for *Hsisosuchus* were derived from the incomplete skeletons of *Hsisosuchus chungkingensis* and *Hsisosuchus dashanpuensis*. All ingroup taxa were coded at the species level (Appendix 3).

Two sets of maximum parsimony search algorithms using tree bisection-reconnection heuristic searches were employed with PAUP* 4.0b10 (Swofford, 2002). Each search used 200 repetitions with randomly added taxa to avoid potential heuristic islands (Maddison, 1991). One set employed all taxa within the data matrix, whereas the other excluded *Trematochampsa* and juvenile *Hamadasuchus*. The former was excluded because of its problematic nature (see below). The latter was excluded to maintain only adult representatives of terminal taxa. In all cases, up to six nonparsimonious heuristic islands were found and avoided using this approach. The strict and Adams consensus trees for the most parsimonious trees are illustrated (Fig. 8). A bootstrap analysis was performed using 2000 bootstrap replicates of the same heuristic search parameters outlined above.

The strict and Adams consensus trees of the two sets of taxa were nearly identical within and between each set (Fig. 8). Tree statistics are presented in the figure legend. Tree topologies are identical with and without *Trematochampsa* and juvenile *Hamadasuchus*. Therefore, because of the problematic nature of *Trematochampsa*, and in an effort to discuss only characters of adult specimens, all following discussions of tree topology and character evolution will reference the reduced taxa trees shown in Figure 8 (C and D). Characters will be discussed as unambiguously optimized and as delayed transformed to account for the degree of missing data inherent with fossil taxa.

The resulting trees indicate a basal position for a monophyletic group Thalattosuchia. This taxon is supported by a suite of synapomorphies listed in Appendix 4. Some of these characters include nasals excluded from the external nares by a maxilla–maxilla contact, elongate supratemporal fenestrae, absence of dorsal and ventral lateral rims on squamosal to support external ear-flap musculature, postorbital lateral to jugal contact on postorbital bar, dentary teeth occlude in line with maxillary teeth, and absence of fourth trochanter on femur. The next most inclusive node consists of Notosuchia and a clade composed of *Araripesuchus*, Neosuchia, and Peirosauridae. This large clade is diagnosed by a number of unique synapomorphies. These include anterior process of jugal approximately twice as broad as posterior process, slender postorbital bar, sagittal extension of premaxilla into external naris more than 10% but less than 50% of narial opening, ectopterygoid contacting postorbital bar, broad quadrate–squamosal contact enclosing cranioquadrate space, posterodorsal crest on quadrate from medial condyle to lateral extent of quadrate–squamosal contact, and square dorsal osteoderms.

Notosuchia (*sensu* Sereno *et al*., 2001) is the sister group to the remaining taxa. Notosuchia is here diagnosed by ten unambiguous and one more delayed transformed synapomorphies. These include relatively smooth, unsculptured skull surface, presence of posterior squamosal prong extending below skull roof and without sculpturing, short preorbital region of skull, anterior orientation of external naris, fewer than ten maxillary teeth, and jaw articulation situated below maxillary tooth row. Unique features of this clade are presence of denticles on teeth, shallow, anteriorly spatulate mandibular symphysis, and mandibular articular cotyle longer than wide.

Araripesuchus gomesii shares eight unambiguous apomorphies with *Baurusuchus*, Neosuchia, and peirosaurids. Five of these synapomorphies are unique to this clade and include presence of circumnarial fossa, third maxillary tooth largest in maxilla, complete midline contact of pterygoids on primary palate covering most of basisphenoid, medial and lateral insertion of musculus pterygoideus posterior on angular, and snout wider than high. *Araripesuchus patagonicus* lacks some of these features, but was placed in a similar phylogenetic position by Ortega *et al*. (2000). Although the post-temporal foramen within the supratemporal fossa is visible in dorsal view in a number of non-neosuchian crocodyliforms, this feature is more exaggerated in *A. patagonicus* and is combined with shallow, poorly developed supratemporal rims. This combination of features are similar to those in extant juvenile crocodylians, such as juveniles of *Alligator sinensis* (Cong, Hou & Wu, 1984), and *Crocodylus porosus*, *Crocodylus niloticus*, *Caiman yacare*, *Caiman latirostris*, and *Alligator mississippiensis* (H. C. E Larsson, pers. observ.). The small size of *A. patagonicus* (anteroposterior skull length approximately 60 mm) compared with that of other species of *Araripesuchus* [anteroposterior skull length approximately 120 mm for *A. gomesii* (Price, 1959) and up to 140 mm for *A. wegeneri* (H. C. E Larsson, pers. observ. of unpublished specimens)] suggests that *A. patagonicus* may indeed be based on juvenile material.

Downloaded from https://academic.oup.com/zoolinnean/article/149/4/533/2630922 by guest on 31 August 2021

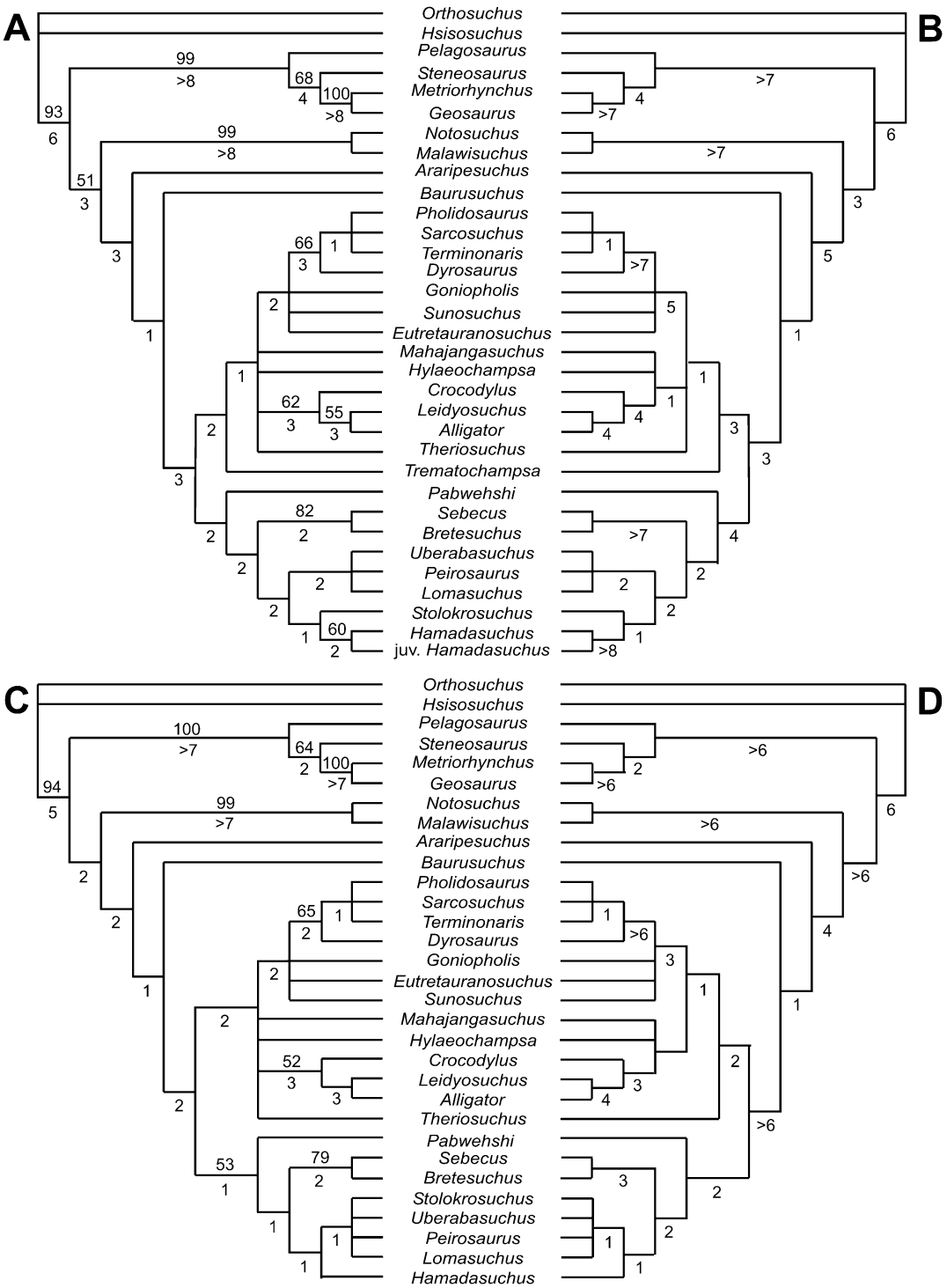

Figure 8. Results of phylogenetic analysis. A, strict consensus of the 48 most parsimonious trees with all taxa included. Tree length is 548 steps, consistency index is 0.3923, retention index is 0.6623, and rescaled consistency index is 0.2598. Bootstrap support values are given above each branch for values greater than 50%. Bremer decay values are given below each branch. B, Adams consensus of the same set of trees with Adams decay values below each branch. C, strict consensus of the 138 most parsimonious trees of the reduced taxon set. Tree length is 540 steps, consistency index is 0.3981, retention index is 0.6546, and rescaled consistency index is 0.2606. Bootstrap support values greater than 50% are presented above each branch and Bremer decay values below each branch. D, Adams consensus of this set of trees with Adams decay values below each branch.

Downloaded from https://academic.oup.com/zoolinnean/article/149/4/533/2630922 by guest on 31 August 2021

An interesting clade composed of *Baurusuchus*, Neosuchia, and Peirosauridae is the sister taxon of *A. gomesii*. Three unambiguous and two more delayed transformed synapomorphies diagnose this clade. Unambiguous synapomorphies are absence of premaxillary labial process, enlarged fourth dentary tooth, gently curved alveolar margin between dentary teeth 3 and 10. Delayed transformed synapomorphies are reduced antorbital fenestra and occlusion of enlarged anterior dentary teeth within laterally open notch within premaxilla–maxilla contact.

Neosuchia and a clade comprising Peirosauridae, Sebecidae, *Pabwehshi*, and *Hamadasuchus* form the next most inclusive clade. The clade is well supported by seven unambiguous and ten delayed transformed synapomorphies. Four of the unambiguous synapomorphies are unique to this clade: presence of at least small spina quadratojugalis, presence of vascular foramen on dorsolateral region of postorbital bar, a double convexity on maxillary alveolar margin, and posteroventral notch within squamosal–quadrate contact within otic aperture. Other unambiguous synapomorphies include narrow interorbital distance across frontals, location of ventral rim of squamosal for external ear-flap musculature directly beneath dorsal rim, and small anteromedial extension of premaxilla into posterior corner of external naris.

We use the name Neosuchia for a clade that comprises a set of relatively poorly resolved taxa but that has high overall clade support (see below). The decreased resolution within the clade may be a result of the large amount of missing data for *Theriosuchus*. *Theriosuchus* is the only member of that clade to drop to the most inclusive neosuchian node when an Adams consensus is calculated, and suggests this is the most erratic taxon within the most parsimonious tree set. Similarly, taxa such as *Mahajangasuchus*, *Hylaeochampsa*, and *Eutretauranosuchus* have relatively large amounts of missing data. However, Neosuchia are diagnosed by 17 unambiguous and five more delayed transformed synapomorphies. Three unambiguous synapomorphies unique to this clade are presence of overhanging bony rims around all but the anteromedial corner of supratemporal fenestra, presence of anterolateral projections from the postorbital bar, and enlarged fourth and fifth maxillary teeth such that either one or both are largest maxillary teeth. Exclusion of the pubis from the acetabulum uniquely diagnoses this clade under delayed transformation. This character, along with a sigmoidal humerus and a tibia shorter than the femur, defend the novel position of *Mahajangasuchus* within this clade. These characters cannot yet be scored for any sebecian and may offer dramatic changes to the phylogenetic position of *Mahajangasuchus*. Buckley & Brochu (1999) presented *Mahajangasuchus insignis* as a sister taxon to Peirosauridae, with admittedly weak support, on the basis of a transversely thick dorsal region of the splenial. This region is currently only known from a specimen referred to *P. torminni* from Argentina (Gasparini, 1982; Gasparini *et al*., 1991). The region is slightly dorsoventrally crushed in that specimen, making the character difficult to score. Carvalho, Ribeiro & Avilla (2004) unite *Uberabasuchus* with *Mahajangasuchus* on the basis of a ventrally sloping posterodorsal margin of the surangular. This particular character, however, is widespread among Crocodyliformes, including sebecians and neosuchians.

The clade that we are calling Neosuchia lacks a formal definition because Neosuchia has most recently been used to refer to the stem-based clade containing all taxa more closely related to *C. niloticus* than to *Notosuchus terrestris* (Sereno *et al*., 2001). Earlier uses of Neosuchia were to describe a clade comprising Atoposauridae, Pholidosauridae, Goniopholididae, Dyrosauridae, *Bernissartia*, and Eusuchia (Benton & Clark, 1988), and these taxa with Thalattosuchia (Clark, 1994). These uses expressedly excluded *Sebecus*, *Baurusuchus*, and *Araripesuchus* from Neosuchia. In keeping with the original use of Neosuchia, we redefine Neosuchia as comprising all taxa more closely related to *C. niloticus* than to *Sebecus icaeorhinus*.

Two well-supported clades are generated within Neosuchia. One, Crocodylia, is composed of *Crocodylus*, *Leidyosuchus*, and *Alligator*. This clade is supported by 17 unambiguous and five delayed transformed synapomorphies. The second clade comprises Goniopholididae, *Dyrosaurus*, and Pholidosauridae, and is supported by 11 unambiguous and three delayed transformed synapomorphies. This clade has been grouped with the other clade of longirostrine crocodyliforms, Thalattosuchia, in virtually all previous phylogenetic analyses. The grouping is potentially a result of the large number of correlated characters of longirostrine forms (Clark, 1994). However, qualitative examinations (e.g. Buffetaut, 1981b) have separated the groups into a distinct Dyrosauridae and a clade of Pholidosauridae plus Goniopholididae. Larsson (2000) found support for a clade of Dyrosauridae and Pholidosauridae, with Goniopholididae as a closely related taxon, and all within Neosuchia. Sereno *et al*. (2001, 2003), and this study have identified a clade containing only these taxa.

The sister group to Neosuchia is a clade including Sebecidae, Peirosauridae, *Pabwehshi*, and *Hamadasuchus*. This clade is diagnosed by three unambiguous synapomorphies that include large neurovascular foramen on palatal premaxilla–maxilla contact, premaxillary palatal shelves not meeting posteriorly, and the presence of a sagittal torus on maxillary palatal shelves. The first two character states are found on the type material of *S. icaeorhinus*, but no palatal shelves

Downloaded from https://academic.oup.com/zoolinnean/article/149/4/533/2630922 by guest on 31 August 2021

of the maxillae are preserved to indicate either the presence or the absence of a sagittal torus. The high degree of missing data for *Pabwehshi*, which is only known from the anterior region of a snout and mandible, may be a factor for the number of diagnostic characters for this node. *Pabwehshi* is the sister taxon to a grouping composed of a clade of sebecids and another comprising Peirosauridae and *Hamadasuchus*. Two unambiguous and seven delayed transformed synapomorphies diagnose this large clade. The unambiguous synapomorphies are presence of large, elongate incisive foramen and posteriormost premaxillary alveolus posteriorly excavated by premaxilla–maxilla lateral fossa. An elongate incisive foramen is present in *Sebecus* and at least three of the four peirosaurid taxa, but is transformed to a reduced state in *Hamadasuchus*. The posteriorly excavated last premaxillary alveolus is present in all taxa within this clade that can be coded for this character. Delayed transformed characters that may be a result of the fragmentary nature of the type, and only known specimen, of *Pabwehshi pakistanensis* are deep and elongate depression on prefrontal for reception of palpebral element, posterolateral squamosal prongs that are sculptured and lie level to skull table, ectopterygoid extending along entire edge of pterygoid flange, hypertrophied ventral extension of exoccipital adjacent to basioccipital tubera, and posterodorsal projection of retroarticular process. A unique character found only in this group and optimized under delayed transformation is deep fossa between and behind the first two premaxillary alveoli for reception of enlarged first dentary tooth. Another character diagnosing this clade under delayed transformation is presence of accessory condyle on quadratojugal contributing to mandibular condyle. This character only occurs in one other clade of crocodyliforms, Dyrosauridae, and is unlikely to be homologous to the condition found in sebecids and peirosaurids. All these character-states are present in the taxa within this clade that can be scored for these characters, indicating the states are either synapomorphic for this clade or for this clade and *Pabwehshi*.

The sebecids *Sebecus* and *Bretesuchus* are diagnosed by three unambiguous synapomorphies. These are pointed anterior borders of palatines on secondary palate, snout higher than wide, and the unique feature of median boss or convexity along dorsal surface of rostrum.

The sister taxon to the sebecid taxa is a clade composed of *Hamadasuchus* and a set of four unresolved peirosaurid taxa. This clade is diagnosed by two unambiguous and five delayed transformed synapomorphies. The unambiguous synapomorphies are presence of tall posterior pterygoid process and dorsoventrally elongate posteromedial region of pterygoid subequal in height to basioccipital. Delayed transformed synapomorphies are elongate anterior process of quadratojugal contacting jugal for up to half the length of the lower temporal bar, presence of posteroventral postorbital process extending along anterior margin of quadratojugal, presence of premaxillary labial process, presence of laterosphenoid bridge (which would probably have covered ramus ophthalmicus and a twig of the mandibular branch of nervus trigeminus supplying musculus levator bulbi; Iordansky, 1973), and presence of hemispherical pneumatic recess on anteroventral surface of prefrontal. The latter two characters are, however, sparsely sampled in the matrix.

The four peirosaurid taxa, *Peirosaurus*, *Uberabasuchus*, *Lomasuchus*, and *Stolokrosuchus*, are diagnosed by four unambiguous and one delayed transformed synapomorphy. Unambiguous synapomorphies are separation of lacrimal and nasal by maxilla (although this state is reversed in *Stolokrosuchus* with a broad lacrimal–nasal contact), ovate cross-section of jugal along the lower temporal bar, presence of five premaxillary teeth, the anterior two premaxillary alveoli nearly confluent, and a delayed transformed synapomorphy of anteriorly extended incisive foramen abutting premaxillary tooth row. This latter feature is also present in *Sebecus* and is placed as a synapomorphy for the clade comprising Sebecidae, *Hamadasuchus*, and Peirosauridae under accelerated transformation. The high percentage of missing data for *P. torminni*, as well as the very different skull shapes of the longirostrine *Stolokrosuchus* and the brevirostrine *Lomasuchus*, may account for the difficulty of identifying a large number of synapomorphies at this node.

The numerous characters that diagnose the clade composed of *Pabwehshi*, Sebecidae, Peirosauridae, and *Hamadasuchus*, and its relative stability (see below), have prompted us to designate a name and definition for the clade. Rather than retaining Colbert's (1946) Sebecosuchia, we propose a clade Sebecia derived from the family nomen Sebecidae Simpson 1937. Previous authors have followed Colbert's usage Sebecosuchia to refer to a clade composed of *Sebecus* and *Baurusuchus*. To avoid confusion, we propose Sebecia to name a new clade that does not include *Baurusuchus*. Sebecia is defined here as all crocodyliforms more closely related to *S. icaeorhinus* than to *C. niloticus*. *Sebecus* was chosen as a rooting taxon because it appears to be the first named taxon within the group, has well-described type material, and exhibits many of the characters diagnosing the clade. A unique feature to this clade is the addition of *Sebecus* to the exclusion of *Baurusuchus*. It is interesting to note that Colbert (1946) grouped Sebecidae and Baurusuchidae together as Sebecosuchia on the basis of a deep and narrow snout with laterally directed orbits, a reduction in tooth

Downloaded from https://academic.oup.com/zoolinnean/article/149/4/533/2630922 by guest on 31 August 2021

number, and ziphodont dentition, characteristics that are now known to occur more widely among Crocodylomorpha. These two taxa have generally been grouped as either sister taxa or closely related forms, as they were first included in a phylogenetic analysis by Clark (1994). The characters that supported this grouping were primarily features of the shortened snout, enlarged caniniform teeth, laterally open premaxilla–maxilla fossa for enlarged dentary teeth, in dorsal view sigmoidal dentary tooth row, unconstricted tooth crown–root junctions, serrated teeth, a longitudinal groove on the dentary extending anterior of the external mandibular fenestra, large choanal opening, reduced antorbital fenestra, a deeper than wide snout, and posteriorly orientated retroarticular process (Gasparini *et al*., 1991; Ortega *et al*., 1996, 2000; Buckley & Brochu, 1999; Buckley *et al*., 2000; Brochu *et al*., 2002; Pol, 2003; Sereno *et al*., 2003; Carvalho *et al*., 2004; Turner & Calvo, 2005). Many of these characters are known to be broadly distributed among crocodyliforms. Others, such as the longitudinal groove along the dentary and the size of the choana, are present to varying degrees in numerous taxa and need to be better quantified. Unconstricted tooth crown–root junctions are commonly present in enlarged caniniform teeth in crocodyliforms, whereas the preserved posterior teeth of sebecids have constricted crown–root junctions. When the characters that were deemed informative and observable in a sufficient number of taxa were included in the present analysis, the inclusion of well-documented taxa, such as *Hamadasuchus*, appear to shift the distributions of characters to the resulting phylogenetic hypothesis. Moving *Baurusuchus* to a sister-group relationship with Sebecidae requires 12 additional steps, and moving Sebecidae to a sister-group relationship with *Baurusuchus* requires 15 additional steps.

The close relationship between *Sebecus* and Peirosauridae necessitates definitions for these taxa. Sebecidae, in keeping with the original usage of this nomen by Simpson (1937) and Colbert (1946), is here defined as all taxa more closely related to *S. icaeorhinus* than to *Uberabasuchus terrificus* and *P. torminni*. Peirosauridae is defined as all taxa more closely related to *U. terrificus* and *P. torminni* than to *S. icaeorhinus*. We use *U. terrificus* and *P. torminni* as anchoring taxa in reference to the first described peirosaurid, *Peirosaurus*, and to the well-preserved material of *Uberabasuchus*. Furthermore, it should be noted that the material for *Uberabasuchus* was recovered from the same locality and formation as the type material of *P. torminni*. The structure of the type material of *P. torminni* is indistinguishable from that of *U. terrificus,* and the two taxa have completely overlapping character scores in our data matrix. One feature that was suggested to separate *Uberabasuchus* from *Peirosaurus* is the absence of a significant contribution of the nasals to the internarial bar (Carvalho *et al*., 2004). Instead, these authors interpreted the bar as being composed of a rostral bone, something that would be unique to this taxon and that has not been found in any other crocodylomorph. We suggest that the rostral bone is more likely to be the anterior region of nasals contributing to the internarial bar, as in *Hamadasuchus*, *Stolokrosuchus* (Larsson & Gado, 2000), and interpreted for the type material of *P. torminni* (Price, 1955). We chose to redefine Peirosauridae to better reflect its equivalent taxonomic status to Sebecidae and to honour the early discoveries of *Sebecus* and *Peirosaurus*. A taxonomic arrangement is presented in Figure 9.

Phylogenetic robustness

The matrix was subjected to bootstrapping 2000 times with ten heuristic search replicates for each bootstrap to avoid heuristic islands. Bootstrap supports are indicated in Figure 8. Two clades are not represented in the consensus trees but have significant bootstrap support. A clade of *Goniopholis* plus *Eutretauranosuchus* is supported by 71% and 69% in the complete and reduced taxon sets, respectively. Another clade of *Hylaeochampsa* plus Crocodylia is supported by 75% in both taxon sets. The data were also submitted to a Bremer decay analysis (Bremer, 1988) and a novel approach using Adams consensus trees (Figure 8). Adams consensus trees were used to establish which taxa may be the least stable while conserving stable clade arrangements (Adams, 1972). This approach was used to better accommodate the large degree of missing data found in palaeontological data sets. Wild-card taxa are pulled to more inclusive nodes, and stable arrangements of taxa at less inclusive nodes are retained. When employed with relaxed parsimony searches, Adams consensus trees yield a set of clade decays in a similar manner as strict consensus trees of relaxed parsimony searches yield Bremer decays. For simplicity, we will refer to decays employing Adams consensus trees as Adams decays. Like Bremer decays, we use the tree length of the Adams consensus at which the clade is no longer retained minus the most parsimonious tree length to obtain an Adams decay value. Adams decays, however, are not additive like Bremer decays. The nature of Adams condenses may result in the loss of a stable clade at low levels of relaxed parsimony, but the re-establishment of that clade at higher levels of relaxed parsimony resulting from the rearrangements of other, unrelated taxa within the tree. The values indicated in Figure 8 are the maximum Adams decay values. Further exploration of the use of Adams decays is beyond the scope of this work, but will be discussed elsewhere by H. C. E. Larsson.

Downloaded from https://academic.oup.com/zoolinnean/article/149/4/533/2630922 by guest on 31 August 2021

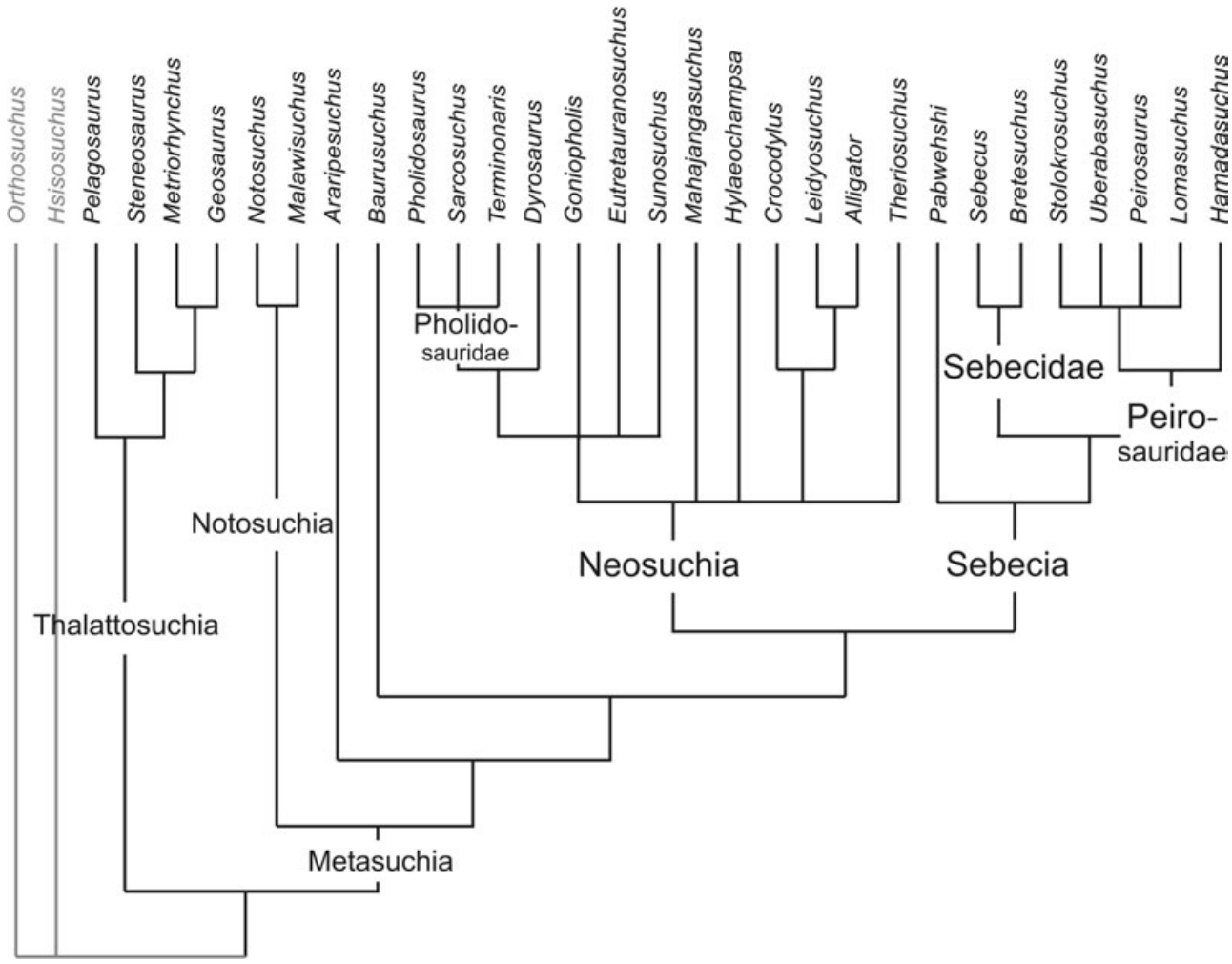

Figure 9. Taxonomic arrangement of Mesosuchia based on Fig. 8C.

Like many fossil-based phylogenetic analyses, the consensus trees lost significant resolution after the addition of only two steps – the most common problem in phylogenetic analyses of crocodylomorphs caused by missing data and high levels of homoplasy. Bremer decay values are highest for the ingroup clade, Thalattosuchia, *Metriorhynchus* plus *Geosaurus*, and Notosuchia (Fig. 8A–C). Moderate Bremer decay values support Crocodylia and the clade comprising Neosuchia plus Sebecia when *Trematochampsa* is included in the analysis. This variability suggests that there are characters with high homoplasy near this node, and this must be addressed with additional well-preserved taxa.

Adams decay values are generally higher than the Bremer decay values because of the omission of wildcard taxa from consensus topologies. In addition to the well-supported nodes in the Bremer decay analysis, Adams decay values give strong support for the clades of *Dyrosaurus* plus Pholidosauridae, Goniopholididae plus *Dyrosaurus* plus Pholidosauridae, Sebecia, Sebecidae, and *Hamadasuchus* when the juvenile specimens are scored as a separate operational taxonomic unit (OTU). Adams decay values also support clades not represented in the consensus trees. *Sarcosuchus* and *Terminonaris* have Adams decay values of four in both taxonomic sets. A clade of Crocodylia plus *Hylaeochampsa* (= Eusuchia) has Adams decay values of greater than seven in the total taxonomic set, and greater than six in the reduced taxonomic set. The goniopholidid taxa are supported as a clade in the reduced taxonomic set with Adams decay values of four, and *Goniopholis* and *Eutretauranosuchus* are supported as a clade with decay values of five. The majority of other clades have lowered Adams decay values as a result of basal consensus placements of *Pabwehshi* and *Mahajangasuchus*.

Downloaded from https://academic.oup.com/zoolinnean/article/149/4/533/2630922 by guest on 31 August 2021

Character and taxon discussion

Several morphological differences are evident between the various growth stages of *H. rebouli*. Some appear to show ontogenetic change (Fig. 7). The smallest specimen with a preserved skull roof (ROM 52059) has a low but sharp sagittal crest that extends anteriorly from the frontoparietal suture. The anterior region of the crest rises to a height of approximately 2 mm at about the level of the posterior edge of the orbits. The specimen is incomplete anterior to this point. A similarly positioned but greatly reduced crest is present on the next smallest specimen (ROM 54511). The largest specimen (ROM 52620) does not show any trace of the crest. A similar crest is present in *Sebecus*. The crest in this taxon rises to a peak at the frontoparietal suture and becomes reduced at the mid-length of the orbits. *Lomasuchus* has a trace of a sagittal crest in a similar position; however, the crest is too weakly developed to be coded with confidence. As other known taxa do not have a sagittal crest, the character was not included in the character–taxon matrix because it would be uninformative. However, including the character and coding it as present in *Lomasuchus* did not change the number and topology of the most parsimonious trees recovered.

Another feature of the skull roof that appears to show an ontogenetic trend is the raised medial rims of the supratemporal fenestrae. The smallest specimen (ROM 52059) has rims that are nearly 3-mm high. The rims are present in ROM 54511 but reduced in height to approximately 1 mm. Rims are completely absent in ROM 54513 and ROM 52620. Of the taxa included in the present analysis, *Hamadasuchus* appears to be the only sebecian to lose these rims in adult specimens.

The smallest specimens, ROM 52059 and ROM 54511, also have a crest on the posterodorsal surface of the quadrate. The crest extends from the junction between quadrate, squamosal, and paroccipital process to the dorsal edge of the medial mandibular condyle (the distal end is preserved only in ROM 52059). The crest is absent in the larger ROM 52620.

The only remaining ontogenetic difference apparent in the material concerns shape changes in the posterior dentary teeth. The smallest specimen (ROM 52047) has labiolingually compressed ziphodont teeth that are 4.0-mm wide labiolingually and 6.5-mm long mesiodistally at their crown base, or 62% wide as long. Teeth in similar positions in the larger ROM 49282 and ROM 52045 are more robust with a labiolingual width of 9.0 mm and mesiodistal length of 12.5 mm at their crown bases, or 72% wide as long. The more gracile nature of the teeth in the small specimen may suggest a change in diet during ontogeny in this taxon, similar to that reported for many extant crocodylians.

Possible sebecian taxa

Trematochampsa taqueti

The taxonomic identity of the material of the type of *T. taqueti* is problematical. Buffetaut (1976a) described a locality near In Beceten, Niger, that has yielded more than a thousand crocodyliform bones from strata that are between Cenomanian and Turonian ('Senonian') in age. Most of these specimens were elements of the skull and vertebral column. Buffetaut recognized three different crocodyliform taxa from the assemblage: *T. taqueti*, *Libycosuchus* sp., and a large but undiagnosable longirostrine form. The rationale for associating the cranial elements, vertebrae, and some appendicular bones as the hypodigm for the new taxon was not discussed. Various authors have previously questioned the validity of *T. taqueti* and the family Trematochampsidae (see above). The phylogenetic analysis presented in this paper raises further questions concerning the validity of this taxon.

Although clearly not a test of the validity of the taxon, the ambiguous placement of *T. taqueti* in the trees discussed above does hint at the composite nature of its hypodigm. The assigned elements appear to share features associated with different levels of the phylogeny presented here. The absence of a circumnarial fossa, hypertrophied exoccipitals along basioccipital tubera, and the depression on the anterodorsal edge of the postorbital for a palpebral bone indicate that *T. taqueti* is not related to Sebecia. On the other hand, the contribution of the quadratojugal to the mandibular condyle, enlarged penultimate premaxillary tooth, lateral fossa between premaxilla and maxilla excavating last premaxillary alveolus, and fourth dentary tooth larger than third, suggest sebecian affinities. This incongruent combination of features is part of the reason why the position of *T. taqueti* could not be resolved. Another reason is the paucity of osteological data for this taxon. Clearly more work is needed to resolve the phylogenetic position and taxonomic validity of *T. taqueti*. We can only note features that are in conflict with the phylogenetic hypothesis reported here.

Pabwehshi pakistanensis

The holotype and only known specimen of *P. pakistanensis* is a snout preserved back to the second maxillary tooth with the associated rostral end of the mandible. The specimen was recovered from the Upper Cretaceous (Maastrichtian) Pab Formation of Balochistan (Pakistan) (Wilson, Malkani & Gingerich, 2001). *P. pakistanensis* shares numerous features with

Downloaded from https://academic.oup.com/zoolinnean/article/149/4/533/2630922 by guest on 31 August 2021

Sebecia in general and *H. rebouli* in particular, including presence of circumnarial fossa, pinched posterodorsal corner of external naris as a result of hypertrophied premaxillary extension along internarial bar, large contribution of nasal to internarial bar, and presence of sagittal torus on maxillary palatal shelf. The degree of similarity between *P. pakistanensis* and *H. rebouli* indicates a close relationship between these taxa. This relationship is supported by the relatively robust position of *Pabwehshi* as a basal sebecian.

Hamadasuchus-like teeth from India

Teeth described from Maastrichtian-age Inter-Trappean strata of Naskal, India, have been closely allied with *Hamadasuchus* (Prasad & Lapparent de Broin, 2002). The relation was entirely based on tooth shape and serration structure. In a thorough survey of all ziphodont crocodyliforms, Prasad & Lapparent de Broin (2002) suggested the existence of a *Hamadasuchus* group comprising *H. rebouli*, 'aff. *Araripesuchus*' from the Koum Basin of Cameroon, and '*Araripesuchus' wegeneri* from Gadoufaoua, Niger. The latter two forms are Early Cretaceous in age. All three have teeth exhibiting a true ziphodont condition, redefined as 'having anterior and posterior carinae with true denticles well separated from each other and which are clearly not the lateral prolongation of the enamel ridges' (Prasad & Lapparent de Broin, 2002: 60), and their tooth forms are remarkably similar. However, tooth structure in crocodyliforms was shown to be highly homoplastic (Prasad & Lapparent de Broin, 2002), and we would caution against uniting the three aforementioned taxa as a *Hamadasuchus* group.

Moroccan 'Libycosuchus'

Buffetaut (1976b) described an incomplete crocodyliform skull table and quadrate from the Kem Kem beds (Albian–Cenomanian) of Morocco as *Libycosuchus* sp. He also referred an isolated quadrate from Cenomanian rocks near In Beceten, Niger, to *Libycosuchus*. The skull table is close in size to one of the juvenile skull tables of *H. rebouli* (ROM 54511). Buffetaut's illustration of the skull table of the Moroccan '*Libycosuchus*' is reproduced here along with ROM 54511 (Fig. 7). The comparison between the two clearly suggests that the two are conspecific. In fact, many characteristics that diagnose *H. rebouli* are preserved in the Moroccan '*Libycosuchus*' skull table. These include an anteriorly extended supratemporal fossa and a tapered squamosal prong. Juvenile features, such as slightly raised medial rims of the supratemporal fossa and a bony crest extending along the posterodorsal surface of the quadrate from the mandibular condyle to the exoccipital, are also present. The unique quadratojugal participation in the jaw joint is also present and further supports the referral of this specimen to Sebecia.

Biogeographical and evolutionary implications

All known sebecian taxa are from South America, Africa, south-western Europe, and the Indian subcontinent. This distribution suggests a Gondwanan distribution, although no sebecian remains have been recovered from Antarctica and Australia to date. Peirosauridae was previously known from Argentina, Brazil, and Niger (see above), whereas the majority of sebecid diversity is known from South America (Argentina, Bolivia, Brazil, Colombia, and Peru) (Gasparini *et al*., 1993). *Iberosuchus* is known from the Eocene of Portugal and has been interpreted to be closely related to *Sebecus* (Antunes, 1975; Ortega *et al*., 1996). The location of *Hamadasuchus* in Morocco (and perhaps India; Prasad & Lapparent de Broin, 2002) and *Pabwehshi* in Pakistan supports a Gondwanan distribution for the clade Sebecia. *Caririsuchus camposi*, from the Lower Cretaceous Santana Formation of Brazil (Kellner, 1987; Buffetaut, 1991), may also be closely related to *Hamadasuchus*, but most of the holotype has disappeared into a private collection and is no longer available for study. Buffetaut (1991) synonymised *Caririsuchus* with *Itasuchus* Price, 1955 (type-species *Itasuchus jesuinoi* Price, 1955) from the Upper Cretaceous Baurú Formation of Brazil, but offered no character evidence in support of this taxonomic decision.

Despite its phylogenetic cohesiveness, Sebecia exhibits a remarkable range of cranial configurations. The deep-snouted *Hamadasuchus* and *Sebecus* contrast with the relatively broad-snouted *Lomasuchus* and the longirostrine *Stolokrosuchus*. There is nearly as much disparity in skull shape as there is taxonomic diversity within Sebecia. In spite of the great disparity in skull shape, many sebecians appear to have true ziphodont dentition. Further detailed analyses, such as that by Prasad & Lapparent de Broin (2002), are required to clarify the evolution of tooth structure within this group. Clearly much of the fossil record of this clade remains undocumented. Its earliest members are known from Albian–Cenomanian rocks (notwithstanding the possible Early Cretaceous records of 'aff. *Araripesuchus*' from Cameroon and *Caririsuchus* from Brazil). The youngest form appears to be *S. huilensis* from the middle Miocene of Colombia (Langston, 1965). This fossil record indicates a temporal range for this the clade spanning nearly 85 million years. Thus, the high degree of disparity in skull shape should not be surprising for the relatively few known taxa for this clade.

Downloaded from https://academic.oup.com/zoolinnean/article/149/4/533/2630922 by guest on 31 August 2021

ACKNOWLEDGEMENTS

We thank Kevin L. Seymour (Royal Ontario Museum, Toronto) who built this fine collection of material and kindly made it available to us for study. Eberhard Frey (Staatliches Museum für Naturkunde Karlsruhe) assisted in obtaining some of the specimens. William F. Simpson and Gregory A. Buckley (Field Museum), Mark A. Norell (American Museum of Natural History) and Paul C. Sereno (University of Chicago) provided generous access to specimens in their care. The manuscript greatly benefitted from comments from an anonymous reviewer and Diego Pol. This work was supported by funds from Canada Research Chairs and NSERC to HCEL and an NSERC Operating Grant to H-DS.

REFERENCES

Adams EN. 1972. Consensus techniques and the comparison of taxonomic trees. *Systematic Zoology* **21:** 390–397.

Antunes MT. 1975. *Iberosuchus*, crocodile Sebecosuchien nouveau, l'Eocène ibérique au nord de la Chaîne Centrale, et l'origine du canyon de Nazaré. *Comunicaçoes Dos Servicos Geologicos de Portugal* **59:** 285–330.

Benton MJ, Clark JM. 1988. Archosaur phylogeny and the relationships of the Crocodylia. In: Benton MJ, ed. *The Phylogeny and Classification of the Tetrapods*, **Vol. 1***: Amphibians, Reptiles, Birds.* Oxford: Clarendon Press, 295–338.

Bremer K. 1988. The limits of amino-acid sequence data in angiosperm phylogenetic reconstruction. *Evolution* **42:** 795–803.

Brochu CA. 1997. Phylogenetics, taxonomy, and historical biogeography of Alligatoroidea. *Memoirs of the Society of Vertebrate Paleontology* **6:** 9–100.

Brochu CA, Bouaré ML, Sissoko F, Roberts EM, O'Leary MO. 2002. A dyrosaurid crocodyliform braincase from Mali. *Journal of Paleontology* **76:** 1060–1071.

de Broin F, Taquet P. 1966. Découverte d'un Crocodilien nouveau dans le Crétacé inférieur du Sahara. *Comptes Rendus de l'Academie Des Sciences* **262:** 2326–2329.

Buckley GA, Brochu CA. 1999. An enigmatic new crocodile from the Upper Cretaceous of Madagascar. *Special Papers in Palaeontology* **60:** 149–175.

Buckley GA, Brochu CA, Krause DW, Pol D. 2000. A pug-nosed crocodyliform from the Late Cretaceous of Madagascar. *Nature* **405:** 941–944.

Buffetaut E. 1974. *Trematochampsa taqueti*, un Crocodilien nouveau du Sénonien inférieur du Niger. *Comptes Rendus de l'Académie Des Sciences* **279:** 1749–1752.

Buffetaut E. 1976a. Ostéologie et affinités de *Trematochampsa taqueti* (Crocodylia, Mesosuchia) du Sénonien inférieur d'In Beceten (République du Niger). *Géobios* **9:** 143–198.

Buffetaut E. 1976b. Der Land-Krokodilier *Libycosuchus* Stromer und die Familie Libycosuchidae (Crocodylia, Mesosuchia) aus der Kreide Afrikas. *Mitteilungen der Bayerischen Staatssammlung für Paläontologie und Historische Geologie* **16:** 17–28.

Buffetaut E. 1981a. Die biogeographische Geschichte der Krokodilier, mit Beschreibung einer neuen Art, *Araripesuchus wegeneri*. *Geologische Rundschau* **70:** 611–624.

Buffetaut E. 1981b. Radiation évolutive, paléoécologie et biogéographie des crocodiliens mésosuchiens. *Mémoires de la Société Géologique de France*. *Nouvelle Série* **142:** 1–88.

Buffetaut E. 1991. *Itasuchus* Price, 1955. In: Maisey JG, ed. *Santana Fossils: an Illustrated Atlas*. Neptune, NJ: TFH Publications Inc., 348–350.

Buffetaut E. 1994. A new crocodilian from the Cretaceous of southern Morocco. *Comptes Rendus de l'Académie Des Sciences* **319:** 1563–1568.

Buffetaut E, Taquet P. 1977. The giant crocodilian *Sarcosuchus* in the early Cretaceous of Brazil and Niger. *Palaeontology* **20:** 203–208.

Buffetaut E, Taquet P. 1979. An early Cretaceous terrestrial crocodilian and the opening of the South Atlantic. *Nature* **280:** 486–487.

Busbey AB. 1995. The structural consequences of skull flattening in crocodilians. In: Thomason JJ, ed. *Functional Morphology in Vertebrate Paleontology*. New York: Cambridge University Press, 173–192.

Buscalioni AD, Sanz JL, Casanovas ML. 1992. A new species of the eusuchian crocodile *Diplocynodon* from the Eocene of Spain. *Neues Jahrbuch für Geologie und Paläontologie, Abhandlungen* **187:** 1–29.

Carvalho IS, Ribeiro LCB, Avilla LS. 2004. *Uberabasuchus terrificus sp. nov.*, a new Crocodylomorpha from the Bauru Basin (Upper Cretaceous), Brazil. *Gondwana Research* **7:** 975–1002.

Clark JM. 1994. Patterns of evolution in Mesozoic Crocodyliformes. In: Fraser NC, Sues H-D, eds. *The Shadow of the Dinosaurs: Early Mesozoic Tetrapods*. New York: Cambridge University Press, 84–97.

Colbert EH. 1946. *Sebecus*, representative of a peculiar suborder of fossil Crocodilia from Patagonia. *Bulletin of the American Museum of Natural History* **87:** 217–270.

Cong L-P, Hou L-H, Wu X-C. 1984. [Age variation in the skull of *Alligator sinensis* Fauvel in topographic anatomy.] *Acta Herpetologica Sinica* **3:** 1–13. (In Chinese, with English summary.)

Courville P, Meister C, Lang J, Mathey B, Thierry J. 1991. Les corrélations en Téthys occidentale et l'hypothèse de la liaison Téthys-Atlantique Sud: intérêt des faunes d'ammonites du Cénomanien supérieur – Turonien moyen basal du Niger et du Nigeria (Afrique de l'Ouest). *Comptes Rendus de l'Académie Des Sciences* **313:** 1039–1042.

Frey E. 1988. Anatomie des Körperstammes von *Alligator mississippiensis* Daudin. *Stuttgarter Beiträge Zur Naturkunde* **424:** 1–106.

Gasparini Z. 1982. Una nueva familia de cocodrilos zifodontes Cretácicos de América del Sur. *Quinto Congreso Latinoamericano de Geología, Argentina* **Actas IV:** 317–329.

Gasparini Z, Chiappe LM, Fernandez M. 1991. A new Senonian peirosaurid (Crocodylomorpha) from Argentina

Downloaded from https://academic.oup.com/zoolinnean/article/149/4/533/2630922 by guest on 31 August 2021

and a synopsis of the South American Cretaceous crocodilians. *Journal of Vertebrate Paleontology* **11:** 316–333.

Gasparini Z, Fernandez M, Powell J. 1993. New Tertiary sebecosuchians (Crocodylomorpha) from South America: phylogenetic implications. *Historical Biology* **7:** 1–19.

Iordansky NN. 1964. The jaw muscles of the crocodiles and some relating structures of the crocodilian skull. *Anatomischer Anzeiger* **115:** 256–280.

Iordansky NN. 1973. The skull of the Crocodilia. In: Gans C, Parsons TS, eds. *Biology of the Reptilia, Vol. 4: Morphology D.* London and New York: Academic Press, 201–262.

Kellner AWA. 1987. Ocorrência de um novo crocodiliano no Cretáceo Inferior da bacia do Araripe, Nordeste do Brasil. *Anais Da Academia Brasileira de Ciências* **59:** 219–232.

Langston W Jr. 1965. Fossil crocodilians from Colombia and the Cenozoic history of the Crocodilia in South America. *University of California Publications in Geological Sciences* **52:** 1–157.

Lapparent de Broin F. 2002. *Elosuchus*, a new genus of crocodile from the Lower Cretaceous of the North of Africa. *Comptes Rendus Palevology* **1:** 275–285.

Larsson HCE. 2000. Ontogeny and Phylogeny of the Archosauriform Skeleton. PhD Thesis, The University of Chicago.

Larsson HCE, Gado B. 2000. A new Early Cretaceous crocodyliform from Niger. *Neues Jahrbuch für Geologie und Paläontologie, Abhandlungen* **217:** 131–141.

Larsson HCE, Sidor CA. 1999. Unusual crocodyliform teeth from the Late Cretaceous (Cenomanian) of southeastern Morocco. *Journal of Vertebrate Paleontology* **19:** 398–401.

Lavocat R. 1955. Découverté d'un Crocodilien du genre *Thoracosaurus* dans le Crétacé supérieur d'Afrique. *Bulletin Du Muséum National d'Histoire Naturelle* **2:** 338–340.

Maddison DR. 1991. The discovery and importance of multiple islands of most parsimonious trees. *Systematic Zoology* **40:** 315–328.

Norell MA. 1988. Cladistic Approaches to Paleobiology as Applied to the Phylogeny of Alligatorids. PhD Thesis, Yale University.

Norell MA. 1989. The higher level relationships of the extant Crocodylia. *Journal of Herpetology* **23:** 325–335.

Norell MA, Clark JM. 1990. A reanalysis of *Bernissartia fagesi*, with comments on its phylogenetic position and its bearing on the origin and diagnosis of the Eusuchia. *Bulletin de l'Institut Royal des Sciences Naturelles de Belgique*. *Sciences de la Terre* **60:** 115–128.

Ortega F, Buscalioni AD, Gasparini Z. 1996. Reinterpretation and new denomination of *Atacisaurus crassiproratus* (Middle Eocene; Issel, France) as cf. *Iberosuchus* (Crocodylomorpha, Metasuchia). *Géobios* **29:** 353–364.

Ortega F, Gasparini Z, Buscalioni AD, Calvo JO. 2000. A new species of *Araripesuchus* (Crocodylomorpha, Mesoeucrocodylia) from the Lower Cretaceous of Patagonia (Argentina). *Journal of Vertebrate Paleontology* **20:** 57–76.

Pol D. 2003. New remains of *Sphagesaurus huenei* (Crocodylomorpha: Mesoeucrocodylia) from the Late Cretaceous of Brazil. *Journal of Vertebrate Paleontology* **23:** 817–831.

Prasad GVR, Lapparent de Broin F. 2002. Late Cretaceous crocodile remains from Naska (India): comparisons and biogeographic affinities. *Annales de Paléontologie* **88:** 19–71.

Price LI. 1955. Novos crocodilídeos dos arenitos da Série Baurú, Cretáceo do Estado de Minas Gerais. *Anais Da Academia Brasileira de Ciências* **27:** 487–498.

Price LI. 1959. Sôbre un crocodilídeo notossúquio do Cretácico Brasileiro. *Divisão de Geologia E Mineralogia, Departamento Nacional de Produção Mineral (Rio de Janeiro), Boletim* **188:** 1–55.

Russell DA. 1996. Isolated dinosaur bones from the Middle Cretaceous of the Tafilalt, Morocco. *Bulletin Du Muséum National d'Histoire Naturelle* **4:** 349–402.

Sereno PC. 1991. Basal archosaurs: phylogenetic relationships and functional implications. *Memoirs of the Society of Vertebrate Paleontology* **2:** 1–53.

Sereno PC, Dutheuil DB, Iarochene M, Larsson HCE, Lyon GH, Magwene PM, Sidor CA, Varricchio DJ, Wilson JA. 1996. Predatory dinosaurs from the Sahara and Late Cretaceous faunal differentiation. *Science* **272:** 986–991.

Sereno PC, Larsson HCE, Sidor CA, Gado B. 2001. The giant crocodyliform *Sarcosuchus* from the Cretaceous of Africa. *Science* **294:** 1516–1519.

Sereno PC, Sidor CA, Larsson HCE, Gado B. 2003. A new notosuchian from the Early Cretaceous of Niger. *Journal of Vertebrate Paleontology* **23:** 477–482.

Shute CCD, Bellairs Ad'A. 1955. The external ear in Crocodilia. *Proceedings of the Zoological Society of London* **124:** 741–748.

Simpson GG. 1937. New reptiles from the Eocene of South America. *American Museum Novitates* **927:** 1–3.

Stromer E. 1914. Ergebnisse der Forschungsreisen Prof. E. Stromers in den Wüsten Ägyptens. II. Wirbeltier-Reste der Baharîje-Stufe (unterstes Cenoman). 1. Einleitung und 2. *Libycosuchus*. *Abhandlungen der Königlich Bayerischen Akademie der Wissenschaften, Mathematisch-Physikalische Klasse* **27:** 1–16.

Stromer E. 1925. Ergebnisse der Forschungsreisen Prof. E. Stromers in den Wüsten Ägyptens. II. Wirbeltier-Reste der Baharîje-Stufe (unterstes Cenoman). 7. *Stomatosuchus inermis* Stromer, ein schwach bezahnter Krokodilier und 8. Ein Skelettrest des Pristiden *Onchopristis numidus* Haug sp. *Abhandlungen der Bayerischen Akademie der Wissenschaften, Mathematisch-Naturwissenschaftliche Abteilung* **30:** 1–22.

Stromer E. 1933. Ergebnisse der Forschungsreisen Prof. E. Stromers in den Wüsten Ägyptens. II. Wirbeltier-Reste der Baharîje-Stufe (unterstes Cenoman). 12. Die procölen Crocodilia. *Abhandlungen der Bayerischen Akademie der Wissenschaften, Mathematisch-Naturwissenschaftliche Abteilung, Neue Folge* **15:** 1–55.

Stromer E. 1936. Ergebnisse der Forschungsreisen Prof. E. Stromers in den Wüsten Ägyptens. VII. Baharîje-Kessel und -Stufe mit deren Fauna und Flora. Eine ergänzende Zusammenfassung. *Abhandlungen der Bayerischen Akademie der Wissenschaften, Mathematisch-Naturwissenschaftliche Abteilung, Neue Folge* **33:** 1–102.

Downloaded from https://academic.oup.com/zoolinnean/article/149/4/533/2630922 by guest on 31 August 2021

Swofford DL. 2002. *Paup* Phylogenetic Analysis Using Parsimony (*and Other Methods), Version 4.* Sunderland, Massachusetts: Sinauer Associates.

Taquet P. 1976. Géologie et Paléontologie Du Gisement de Gadoufaoua (Aptien Du Niger) *Cahiers de Paléontologie. Éditions du Centre National de la Recherche Scientifique*, 1–191.

Turner AH, Calvo JO. 2005. A new sebecosuchian crocodyliform from the Late Cretaceous of Patagonia. *Journal of Vertebrate Paleontology* **25:** 87–98.

Whetstone KN, Whybrow PJ. 1983. A 'cursorial' crocodilian from the Triassic of Lesotho (Basutoland), southern Africa. *Occasional Papers of the Museum of Natural History, University of Kansas* **106:** 1–37.

Wilson JA, Malkani MS, Gingerich PD. 2001. New crocodyliform (Reptilia, Mesoeucrocodylia) from the Upper Cretaceous Pab Formation of Vitakri, Balochistan (Pakistan). *Contributions from the Museum of Paleontology, the University of Michigan* **30:** 321–336.

Witmer LM. 1997. The evolution of the antorbital cavity of archosaurs: a study in soft-tissue reconstruction in the fossil record with an analysis of the function of pneumaticity. *Memoirs of the Society of Vertebrate Paleontology* **3:** 1–73.

Wu X-C, Chatterjee S. 1993. *Dibothrosuchus elaphros*, a crocodylomorph from the Lower Jurassic of China and the phylogeny of the Sphenosuchia. *Journal of Vertebrate Paleontology* **13:** 58–89.

Wu X-C, Sues H-D. 1996. Anatomy and phylogenetic relationships of *Chimaerasuchus paradoxus*, an unusual crocodyliform reptile from the Lower Cretaceous of Hubei, China. *Journal of Vertebrate Paleontology* **16:** 688–702.

Wu X-C, Brinkman DB, Lü J-C. 1994. A new species of *Shantungosuchus* from the Lower Cretaceous of Inner Mongolia (China), with comments on *S. chuhsiensis* Young, 1961 and the phylogenetic position of the genus. *Journal of Vertebrate Paleontology* **14:** 210–229.

Wu X-C, Sues H-D, Dong Z. 1997. *Sichuanosuchus shuhanensis*, a new Early Cretaceous protosuchian (Archosauria: Crocodyliformes) and the monophyly of Protosuchia. *Journal of Vertebrate Paleontology* **17:** 89–103.

APPENDIX 1

ANATOMICAL ABBREVIATIONS

bo, basioccipital; bs, basisphenoid; d, dentary; eo, exoccipital; ec, ectopterygoid; f, frontal; j, jugal; l, lacrimal; m, maxilla; n, nasal; p, parietal; pl, palatine; pm, premaxilla; po, postorbital; prf, prefrontal; pt, pterygoid; q, quadrate; qj, quadratojugal; soc, supraoccipital; sp., splenial; sq, squamosal; v?, possible vomer.

APPENDIX 2

CHARACTER DESCRIPTIONS

A total of 158 characters and character-states were used in the phylogenetic analysis. Individual characters and character-states are described below. The character–taxon matrix is presented in Appendix 3. Characters 1, 6, 9, 10, 12, 18, 19, 27, 28, 31, 38, 39, 41, 49, 50, 54, 72, 73, 79, 81, 83, 84, 89, 90, 95, 96, 98, 100, 107, 119, 122, 126, 138, 141, 152, 153, and 157 were treated as ordered, but all others are unordered. Characters are either adapted from previously published analyses or are new. The previously published characters are indicated with reference to either the first or more relevant use of that character in square brackets.

1. Nasal extension dorsally into external naris: (0) absent by maxilla–maxilla contact; (1) absent by premaxilla–premaxilla contact; (2) none but contacts external naris; (3) present and less than 50%; (4) present and more than 50% but not completely. [Larsson (2000)]
2. Dorsal surface of rostrum: (0) curves smoothly; (1) with median boss. [Adapted from Brochu (1997)]
3. Immediate preorbital region cross-section: (0) squared; (1) gently curved. [Larsson (2000)]
4. Prefrontal and lacrimal orbital margin: (0) flat; (1) dorsally upturned to telescope orbit. [Larsson (2000)]
5. Orbital margin of prefrontal: (0) confluent with orbit; (1) projecting laterally. [Larsson (2000)]
6. Depression on prefrontal for palpebral element: (0) absent; (1) thin groove; (2) deep groove terminating anteriorly in deep fossa. [Larsson (2000)]
7. Transverse external prefontal–frontal ridge: (0) absent; (1) present and complete over prefrontals and frontals. [Larsson (2000)]
8. Hemispherical pneumatic recess in ventral surface of prefrontal: (0) absent; (1) present.
9. Prefrontal pillar contact with palate: (0) descending process present but not contacting palatines; (1) present but not with a robust suture; (2) present with a robust suture. [Modified from Clark (1994)]
10. Lacrimal–nasal superficial contact: (0) broad contact; (1) maxilla with short posterior processes partially separating lacrimal and nasal; (2) maxilla with a long posterior process completely separating lacrimal and nasal. [Modified from Brochu (1997)]
11. External lacrimal shape: (0) longer than wide; (1) nearly as wide as long. [Modified from Brochu (1997)]
12. Total lacrimal length relative to total prefrontal length: (0) longer; (1) subequal; (2) shorter. [Adapted from Norell (1988)]
13. Anterior ramus of frontal relative to anterior ramus of prefrontal: (0) posterior; (1) anterior. [Larsson (2000)]

Downloaded from https://academic.oup.com/zoolinnean/article/149/4/533/2630922 by guest on 31 August 2021

14. Frontal–frontal contact: (0) paired; (1) fused. [Clark (1994)]
15. Width of frontal between orbits relative to midlength width across nasals: (0) narrow (similar to width of nasals); (1) broad (about twice width of nasals). [Modified from Clark (1994)]
16. Frontal orbital margin: (0) flat; (1) dorsally upturned. [Larsson (2000)]
17. Frontoparietal suture entry into supratemporal fenestra: (0) deep, preventing broad postorbital (or postfrontal)–parietal contact; (1) no entry, broad postorbital (or postfrontal)–parietal contact. [Modified from Clark (1994)]
18. Dermal bone overhang about the supratemporal fenestra: (0) absent; (1) present only medially; (2) present about all but the anteromedial corner (fossa). [Larsson (2000)]
19. Medial borders of supratemporal fenestrae: (0) separated by a broad sculptured region; (1) separated by a thin sculptured region; (2) contact to form a low sagittal crest. [Larsson (2000)]
20. Medial dorsal edges of supratemporal fenestrae: (0) flat; (1) raised.
21. Anteroposterior length of supratemporal fenestrae: (0) either equal to or shorter than orbits; (1) much longer than orbits. [Adapted from Clark (1994)]
22. Posterior extent of orbital edge of jugal: (0) confluent with postorbital bar; (1) displaced laterally and ending anterior to postorbital bar (forming posteroventral notch in orbit); (2) displaced laterally and ending either at or just behind postorbital bar; (3) displaced laterally and ending near posterior corner of infratemporal fenestra. [Larsson (2000), modified from Brochu (1997)]
23. Width of anterior process of jugal relative to posterior process: (0) subequal; (1) about twice as broad. [Adapted from Clark (1994)]
24. Dorsal surface of jugal beneath infratemporal fenestra: (0) ovate cross-section; (1) longitudinal crest. [Modified from Clark (1994)]
25. Anterior process of jugal relative to infratemporal fenestra anteroposterior length: (0) subequal; (1) much longer. [Larsson (2000)]
26. Anterior margins of lacrimal and jugal: (0) confluent with no notch at anterior contact; (1) jugal edge convex producing anterior notch at contact. [Larsson (2000)]
27. Quadratojugal–postorbital contact: (0) absent; (1) narrowing dorsally and contacting small region of postorbital; (2) broadening dorsally to contact most of the postorbital bar reducing infratemporal fenestra. [Modified from Buscalioni, Sanz & Casanovas (1992) and Clark (1994)]
28. Spina quadratojugalis: (0) absent; (1) either small or low crest; (2) prominent. [Adapted from Norell (1989) and Brochu (1997)]
29. Elements at posterior angle of infratemporal fenestra: (0) quadratojugal; (1) quadratojugal–jugal; (2) jugal. [Adapted from Norell (1989)]
30. Quadratojugal contribution to mandibular condyle: (0) absent; (1) present.
31. Length of anterior process of quadratojugal: (0) either short or absent; (1) from long (less than half length of lower temporal bar) to moderate (one third of lower temporal bar); (2) long (greater than half of lower temporal bar). [Adapted from Brochu (1997)]
32. Dorsal and ventral rims of squamosal groove for external ear-flap musculature: (0) absent; (1) ventral placed lateral to dorsal; (2) ventral directly beneath dorsal. [Larsson (2000)]
33. Posterior region of auditory fossa: (0) opening posteriorly; (1) bounded posteriorly by posteroventrolateral extension of squamosal and exoccipital.
34. Posterior skull table: (0) nonplanar (squamosal ventral to horizontal level of postorbital and parietal); (1) planar (postorbital, squamosal, and parietal on same horizontal plane). [Modified from Clark (1994)]
35. Squamosal prongs: (0) either short or absent; (1) present, depressed from skull table, and unsculptured; (2) present and sculptured and at same level as skull table. [Modified extensively from Clark (1994) and Brochu (1997)]
36. Distal squamosal prong: (0) tapered; (1) broad. [Larsson (2000)]
37. Cranial table width relative to ventral portion of skull: (0) nearly as wide; (1) narrower. [Adapted from Wu *et al*. (1997)]
38. Postorbital bar: (0) transversely flattened (ectopterygoid not strongly contacting bar); (1) massive (roughly anterolateral elliptical cross-section); (2) slender (cylindrical); roughly anteromedially elliptical. [Adapted from Norell (1989) and Clark (1994)]
39. Postorbital posteroventral process: (0) absent; (1) present as slender descending process from postorbital along quadratojugal; (2) present and contacting quadrate. [Modified from Brochu (1997)]
40. Anterolateral projections on postorbital bar: (0) absent; (1) present. [Adapted from Norell (1989)]
41. Anterior extension of external auditory meatus fossa: (0) squamosal; (1) onto posterior margin of postorbital, separated from anterior margin by vertical ridge (postorbital roof overhanging postorbital-squamosal suture); (2) to anterolateral edge of postorbital; (3) along entire length of postorbital and continuing into orbit over thin

Downloaded from https://academic.oup.com/zoolinnean/article/149/4/533/2630922 by guest on 31 August 2021

ramus of postorbital. [Larsson (2000); modified from Brochu (1997)]
42. Position of postorbital relative to jugal on ventral end of postorbital bar: (0) anterior; (1) medial; (2) lateral. [Modified from Clark (1994)]
43. Vascular opening on lateral edge of dorsal part of postorbital bar: (0) absent; (1) present. [Modified from Clark (1994)]
44. Postorbital with prominent anterolateral projection distinct from dorsal corner: (0) absent; (1) present. [Adapted from Clark (1994)]
45. Depression on anterodorsal surface of postorbital for palpebral element: (0) absent; (1) present. [Larsson (2000)]
46. Postorbital bar relative to dorsolateral edge of postorbital: (0) continuous; (1) inset medially. [Adapted from Clark (1994)]
47. Bar between orbit and supratemporal fossa: (0) broad; (1) narrow (fossa nearly covering entire bar). [Adapted from Clark (1994)]
48. Snout (anterior margin of orbit to rostrum) length relative to remainder of skull: (0) longer; (1) shorter. [Adapted from Wu *et al*. (1997)]
49. Premaxilla anterior extension into external naris: (0) none; (1) small projection (less than 10% of the length of naris); (2) present and less than 50%; (3) present and more than 50%, but not completely. [Modified from Clark (1994); Brochu (1997)]
50. Premaxilla extension into external naris from posterior margin of naris: (0) absent; (1) present and thin; (2) present and thick to form posterodorsal notch. [Modified from Larsson (2000)]
51. Premaxillary labial process extending anteriorly beyond tooth row: (0) absent; (1) present. [Larsson (2000)]
52. External nares orientation: (0) either lateral or anterodorsolateral; (1) dorsally; (2) anteriorly. [Modified from Clark (1994)]
53. Circumnarial fossa: (0) absent; (1) present. [Larsson (2000)]
54. Premaxillary tooth count: (0) three; (1) four; (2) five. [Modified from Norell (1988)]
55. Anterior two premaxillary teeth: (0) separate; (1) nearly confluent. [Larsson (2000)]
56. Deep fossa between and behind first and second premaxillary teeth to accommodate enlarged, procumbent first dentary tooth: (0) absent; (1) present.
57. Premaxillary and anterior dentary tooth row orientation: (0) posterolateral; (1) nearly transverse. [Sereno *et al*. (2001)]
58. Anterior premaxillary teeth orientation: (0) vertical; (1) posteriorly inturned. [Sereno *et al*. (2001)]
59. Secondmost posterior premaxillary tooth size relative to anterior premaxillary teeth: (0) similar; (1) much longer. [Modified from Clark (1994)]
60. Large nutrient foramen on palatal surface of premaxilla–maxilla contact: (0) small of absent; (1) large.
61. Premaxilla palatal shelves: (0) not meeting posteriorly; (1) meeting posteriorly.
62. Incisive foramen: (0) present and large (length either equal to or more than half the greatest width of premaxillae); (1) present and small (length less than half the width of the premaxillae); (2) absent (palatal parts of premaxillae in contact along entire length. [Modified from Clark (1994) and Brochu (1997)]
63. Anteromedial extension of incisive foramen: (0) far from premaxillary tooth row (level of either second or third alveolus); (1) abutting premaxillary tooth row. [Adapted from Brochu (1997)]
64. Posterodorsal premaxillary process extension: (0) not beyond third maxillary alveolus; (1) beyond third maxillary alveolus. [Adapted from Brochu (1997)]
65. Enlarged anterior dentary teeth occlusion at premaxilla–maxilla suture: (0) enlarged teeth absent; (1) lingually within internal fossa (fossa may extend dorsally to form foramen); (2) labially within laterally open notch. [Modified from Norell (1988)]
66. Premaxilla–maxilla lateral fossa excavating alveolus of last premaxillary tooth: (0) no; (1) yes.
67. Maxillary tooth number: (0) ten or more; (1) less than ten. [Sereno *et al*. (2003)]
68. Ornamentation on carinae of maxillary and opposing dentary teeth: (0) smooth; (1) serrations; (2) denticles. [Modified from Sereno *et al*. (2003)]
69. Largest maxillary alveolus: (0) maxillary teeth homodont; (1) three; (2) four; (3) four and five; (4) five. [Modified from Norell (1988) and Brochu (1997)]
70. Maxilla–maxilla contact on palate: (0) only posterior ends not in contact at sutures with palatines; (1) complete. [Adapted from Clark (1994)]
71. Sagittal torus on maxillary palatal shelves: (0) absent; (1) present.
72. Antorbital fenestra size relative to orbit: (0) about half; (1) smaller than half but present; (2) only an external fossa (may have tiny fenestra); (3) absent. [Modified from Clark (1994) and Wu *et al*. (1997)]
73. Ventrolateral edge of maxilla: (0) straight; (1) single convexity; (2) double convexity ('festooned'). [Modified from Clark (1994)]

Downloaded from https://academic.oup.com/zoolinnean/article/149/4/533/2630922 by guest on 31 August 2021

74. Posterior extent of maxilla: (0) posterior to anterior margin of orbit; (1) anterior to anterior margin of orbit. [Adapted from Wu & Chatterjee (1993)]
75. Maxillary depression (separate from antorbital fenestra) on lateral surface near lacrimal: (0) absent; (1) present. [Adapted from Wu *et al*. (1997)]
76. Palatine–pterygoid suture on secondary palate relative to posterior angle of suborbital fenestra: (0) nearly at angle; (1) far from it. [Adapted from Brochu (1997)]
77. Posterolateral edges of palatines on secondary palate: (0) parallel; (1) flare laterally to form shelf. [Adapted from Norell (1988)]
78. Anterior process of palatine on secondary palate: (0) pointed; (1) rounded; (2) wide and squared (flat anteriorly). [Adapted from Brochu (1997)]
79. Palatine secondary palate: (0) palatines forming palatal shelves that do not meet; (1) palatal shelves of palatines meeting along anterior two thirds of secondary palate (posteriorly open V – may be filled with pterygoids); (2) palatal shelves of palatines meeting along entire length (straight palatine–pterygoid contact). [Modified extensively from Clark (1994)]
80. Anterior palatal fenestrae on secondary palate: (0) absent; (1) present. [Wu *et al*. (1997)]
81. Pterygoid secondary palate: (0) absent; (1) thin shelves not meeting; (2) secondary palate with anterior margin of choanae located in anterior half of pterygoid length; (3) secondary palate with anterior margin of choanae located in posterior half of pterygoid length. [Modified from Clark (1994)]
82. Choanae projection: (0) posteroventrally into midline depression; (1) ventrally from palate. [Adapted from Clark (1994)]
83. Posterior pterygoid processes: (0) ridges either absent or low; (1) present and near level of palate; (2) present and tall. [Modified from Larsson (2000)]
84. Combined pterygoid width on secondary palate: (0) longer than wide; (1) wider than long but not more than approximately two times wider than long; (2) wider than long and more than two times wider than long. [Larsson (2000)]
85. Pterygoid septum into choanae: (0) absent; (1) present. [Modified from Clark (1994)]
86. Quadrate ramus of pterygoid in ventral aspect: (0) short and broad; (1) short and narrow. [Adapted from Wu *et al*. (1997)]
87. Quadrate ramus of pterygoid: (0) extending dorsally to laterosphenoid; (1) extending dorsally to laterosphenoid and forming ventrolateral edge of trigeminal foramen. [Modified from Clark (1994)]
88. Pterygoids posterior to choanae: (0) paired; (1) fused. [Adapted from Clark (1994)]
89. Pterygoid–pterygoid contact on primary palatal plane: (0) complete to basipterygoid processes (but open posteriorly forming V over basisphenoid); (1) complete with basisphenoid length approximately one third of width; (2) complete with basisphenoid nearly concealed by pterygoid–basioccipital contact. [Modified extensively from Clark (1994)]
90. Posteromedial region of pterygoid in occipital aspect: (0) not visible; (1) visible but less than basioccipital height; (2) visible and subequal in height to basioccipital. [Modified from Brochu (1997)]
91. Ectopterygoid–maxilla contact: (0) absent; (1) present but ectopterygoid only abutting maxilla; (2) present and ectopterygoid near maxillary tooth row; (3) present and broadly separated from tooth row by maxilla. [Modified from Norell (1988) and Brochu (1997)]
92. Ectopterygoid relation to postorbital bar: (0) no support; (1) contributing to base of bar. [Adapted from Clark (1994)]
93. Ectopterygoid extension along lateral pterygoid flange: (0) not to posterior tip of pterygoid; (1) to posterior tip of pterygoid. [Modified from Norell (1988)]
94. Posterior ectopterygoid process along ventral surface of jugal: (0) absent; (1) very small. [Larsson (2000)]
95. Squamosal–quadrate contact within otic aperture posteriorly bounding external auditory meatus: (0) absent; (1) present with smooth posteroventral margin bordering otic aperture; (2) present with posteroventral notch in contact. [Larsson (2000), adapted in part from Brochu (1997)]
96. Quadrate–squamosal–otoccipital contact enclosing cranioquadrate space: (0) absent; (1) present near lateral edge of skull; (2) present with quadrate–squamosal contact broad laterally. [Adapted from Clark (1994)]
97. Prominent crest on dorsal surface of distal quadrate extending proximally to lateral extent of quadrate–exoccipital contact: (0) absent; (1) present. [Modified from Brochu (1997)]
98. Preotic siphonial foramina: (0) absent; (1) single; (2) three or more. [Adapted from Clark (1994)]
99. Dorsal primary head of quadrate contact: (0) only squamosal; (1) squamosal and (or near) laterosphenoid. [Adapted from Clark (1994)]
100. Quadrate–basisphenoid contact: (0) dorsolateral contact; (1) dorsolateral and anterolateral contact. [Modified from Wu *et al*. (1997)]

Downloaded from https://academic.oup.com/zoolinnean/article/149/4/533/2630922 by guest on 31 August 2021

101. Distal quadrate relative to quadrate body: (0) distinct; (1) indistinct – ventromedial contact of quadrate body with otoccipital. [Adapted from Wu, Brinkman & Lü (1994)]
102. Jaw articulation (quadrate condyle), position relative to maxillary tooth row: (0) either above or near level; (1) below. [Wu & Sues (1996)]
103. Laterosphenoid bridge: (0) absent; (1) at least partially complete. [Modified from Brochu (1997)]
104. Prominent boss on paroccipital process: (0) either absent or reduced; (1) present. [Adapted from Brochu (1997)]
105. Ventromedial portion of exoccipital adjacent to basioccipital tuber: (0) slender; (1) hypertrophied. [Larsson (2000)]
106. Large ventrolateral region of paroccipital process: (0) present; (1) absent. [Adapted from Clark (1994)]
107. Supraoccipital exposure on dorsal skull table: (0) absent; (1) small; (2) large. [Adapted from Norell (1988) and Brochu (1997)]
108. Mastoid antrum: (0) extending into fossa in supraoccipital; (1) extending through complete transverse canal in supraoccipital. [Adapted from Clark (1994)]
109. Posterior surface of supraoccipital: (0) nearly flat; (1) bilateral posterior prominences. [Adapted from Clark (1994)]
110. Basioccipital tuberosities: (0) not well developed; (1) large and pendulous. [Adapted from Clark (1994)]
111. Mandibular symphysis depth: (0) deep; (1) shallow and anteriorly spatulate. [Wu & Sues (1996)]
112. Alveolar size for dentary teeth 3 and 4: (0) nearly equal; (1) fourth larger than third. [Modified from Brochu (1997)]
113. Dentary tooth margin curvature between teeth 3 and 10: (0) straight; (1) gently curved. [Adapted from Brochu (1997)]
114. Denary teeth occlusion relative to maxillary teeth: (0) all lingual; (1) in line. [Brochu (1997)]
115. Angular–surangular suture relative to medial wall of external mandibular fenestra: (0) continuing to posterior angle; (1) passing along posteroventral margin. [Adapted from Norell (1988)]
116. Insertion area for musculus pterygoideus posterior on angular: (0) medial; (1) medial and lateral. [Adapted from Clark (1994)]
117. Anterior processes of surangular: (0) one; (1) two. [Adapted from Brochu (1997)]
118. Surangular extension toward posterior end of retroarticular process: (0) along entire length; (1) pinched off anterior to posterior tip. [Adapted from Norell (1988)]
119. External mandibular fenestra: (0) absent; (1) small and foramen intermandibularis caudalis not visible laterally; (2) large and foramen intermandibularis caudalis visible laterally. [Adapted from Norell (1988) and Brochu (1997)]
120. Surangular–articular suture orientation within glenoid fossa: (0) anteroposteriorly (straight); (1) bowed strongly laterally. [Adapted from Brochu (1997)]
121. Articular cotyle of lower jaw: (0) wider than long; (1) longer than wide. (Wu & Sues, 1996)
122. Retroarticular process: (0) short, less than twice the length of the articular cotyle; (1) elongate, either equal to or more than twice the length of the articular cotyle. [Adapted from Benton & Clark (1988) and Norell & Clark (1990)]
123. Medial edge of retroarticular process: (0) either concave or straight; (1) convex. [Larsson (2000)]
124. Projection of retroarticular process: (0) either posteriorly or posteroventrally; (1) posterodorsally. [Adapted from Clark (1994)]
125. Prearticular: (0) present; (1) absent (fused to articular). [Adapted from Clark (1994)]
126. Splenial involvement in mandibular symphysis: (0) not involved; (1) involved for five or less alveoli; (2) involved for more than five alveoli. [Adapted from Clark (1994) and Brochu (1997)]
127. External surface of skull: (0) relatively smooth; (1) heavily sculptured. [Clark (1994)]
128. Snout relative to head width at orbits: (0) abruptly broadening; (1) gradually broadening. [Adapted from Clark (1994)]
129. Snout height and width: (0) higher than wide; (1) equally high as wide; (2) wider than high. [Adapted from Clark (1994)]
130. Axial neural spine height: (0) high, subequal to centrum height; (1) low, less than half centrum height and nearly horizontal. [Larsson (2000)]
131. Axis neural arch lateral process (diapophysis): (0) absent; (1) present. [adapted from Norell (1989) and Brochu (1997)]
132. Cervical vertebrae: (0) either amphicoelous or amphiplatyan; (1) procoelous. [Adapted from Clark (1994)]
133. Dorsal vertebrae: (0) either amphicoelous or amphiplatyan; (1) procoelous. [Adapted from Benton & Clark (1988) and Norell & Clark (1990)]
134. Caudal vertebrae: (0) either all amphicoelous or amphiplatyan; (1) first caudal vertebra gently biconvex and other caudals procoelous. [Adapted from Norell & Clark (1990)]
135. Anterior and posterior margins of scapula in lateral aspect: (0) symmetrically concave in lateral view; (1) anterior edge more strongly concave

Downloaded from https://academic.oup.com/zoolinnean/article/149/4/533/2630922 by guest on 31 August 2021

than posterior edge. [Adapted from Benton & Clark (1988)]
136. Deltoid crest of scapula: (0) present; (1) absent. [Adapted from Brochu (1997)]
137. Scapulocoracoid facet anterior to glenoid fossa: (0) uniformly narrow; (1) broad immediately anterior to glenoid fossa and tapering anteriorly. [Adapted from Brochu (1997)]
138. Coracoid length relative to scapula: (0) half; (1) subequal. [Adapted from Clark (1994)]
139. Proximomedial articular surface on humerus: (0) present (strongly arched edge); (1) absent (weakly arched edge). [Modified from Sereno (1991)]
140. Longitudinal axis of humeral shaft in lateral aspect: (0) straight; (1) sigmoid (distal end curving anteriorly). [Larsson (2000)]
141. Radiale and ulnare length: (0) short (endochondral); (1) long (perichondral); (2) long with distinct proximomedial process on radiale. [Modified from Benton & Clark (1988)]
142. Dorsal margin of iliac blade: (0) rounded with smooth border; (1) flat. [Modified from Brochu (1997)]
143. Posterior iliac process: (0) dorsoventrally expanded with blunt end; (1) nearly absent. [Larsson (2000)]
144. Contribution of pubis to acetabulum: (0) partially excluded by anterior process of ischium; (1) completely excluded from acetabulum. [Clark (1994)]
145. Fibular articular facet of femur: (0) large; (1) very small. [Adapted from Clark (1994)]
146. Lateral edge of proximal articular surface of femur (lesser trochanter): (0) rounded; (1) 'squared' with enlarged scar for musculus ischiotrochantericus. [Larsson (2000)]
147. Fourth trochanter on femur: (0) absent; (1) present but low. [Modified from Sereno (1991)]
148. Tibia length relative to femur length: (0) either subequal or longer; (1) shorter. [Adapted from Sereno (1991)
149. Calcaneal facet for fibula and distal tarsal 4: (0) separate; (1) contiguous. [Sereno (1991)]
150. Calcaneal tuber: (0) either absent or rudimentary; (1) 45° posterolaterally; (2) posteriorly. [Adapted from Sereno (1991) and Parrish (1993)]
151. Fore- and hindlimb lengths: (0) hindlimb much longer than forelimb; (1) subequal.
152. Number of dorsal osteoderms per transverse row: (0) none (dorsal osteoderms absent); (1) two; (2) four or more. [Adapted from Norell & Clark (1990)]
153. Dorsal osteoderm shape: (0) either square or equant; (1) wider than long but less than three times wider than long; (2) more than three times wider than long. [Modified from Norell & Clark (1990) and Brochu (1997)]
154. Anterior edge of dorsal osteoderms: (0) straight; (1) with anterolateral process on anterior edge. [Adapted from Norell & Clark (1990)]
155. Dorsal osteodermal keeling: (0) absent; (1) present. [Adapted from Buscalioni *et al*. (1992)]
156. Dorsal trunk osteoderm, anteroposterior keel position: (0) either medial or paramedian; (1) lateral margin. [Sereno *et al*. (2002)]
157. Ventral trunk osteoderms: (0) absent; (1) present and osteoderms single; (2) present and osteoderms paired ossifications and sutured together. [Adapted from Buscalioni *et al*. (1992)]
158. Tail osteoderms: (0) absent; (1) dorsal only; (2) tail completely surrounded. [Adapted from Clark (1994)]

APPENDIX 3

Character–taxon matrix

Data matrix of 158 characters coded for two outgroups and 25 ingroup taxa. Missing data are shown as '?', and multiple states are indicated within parentheses. Two possible states, used to exclude at least one or more other states within a multistate character, are designated within curly brackets. This designation was used to distinguish an uncertain character-state for taxa in which at least one other of the states was known not to exist, but the nature of the remaining states was uncertain.

Orthosuchus stormbergi
40000{12}0?0? ?100100000 00010??020 0101200000 0100100110 1001000010 0--02-1?00 -0000---0- 0-0-10? 000 0011000210 1000-00?00 011000012? 0???001010 0000100000 2000101012 111111??

Hsisosuchus
4000020?00 0000100010 0001012010 ?201201000 100 0000011 1002000010 12-0??0140 -0111---0- 0-0-1001 00 001?110110 0000-00100 0?00?0001? 0010?2101? ?00010?0?1 2???1????? 11101012

Pelagosaurus typus
0010000?00 0001100010 1000001000 10000-0000 020 0000000 010??000?? ??????0001 0100010111 000-1101 00 0001110001 0000000001 0?0110??2? 0101021110 10001??1?? 11001?011{12} 01100-11

Steneosaurus durobrivensis
0010000?00 000110002- 1000000000 10000-0000 0200000000 0201100010 11002-0001 0100000010

Downloaded from https://academic.oup.com/zoolinnean/article/149/4/533/2630922 by guest on 31 August 2021

001-01?000 1000110?01 10?1000?11 0001?00021 0101020111 0000011100 1100100111 01111011

Metriorhynchus superciliosum
0010100?10 0101100010 1000000000 10000-0000 0200010001 0100000000 01000-0001 0100010120 000-110100 00-0110001 1001000?11 0001-0000? 0001020111 1000011110 0010000101 00----00

Geosaurus suevicus
0010100??0020110002- 100010?000 10000-0000 0200010000 010000000? ???00-0001 03000????? ?????????? ?????10?0? ?0???00?01 0001-00?0? 00?1?20111 1000011110 0010000100 00----00

Pholidosaurus decipiens
0011000??000111?0001 021000{01}?00 12111111?? {12}1?10100?? ?????????? ???1??0001 03000?0?10 1012?1 ?110 110?{12}20011 00?1?10?0? ??01?????? 0????2101? ???????1?? ?????????? ?121111?

Sarcosuchus imperator
1011000010 0011110000 0110000-00 1211111101 {12}101010000 0102001110 11011-0001 0300000110 101211111? 110?220011 0001?10?10 0000101111 011 012111? ?00010???? ?101?????? ?121111{12}

Terminonaris robusta
101?0000?000111-001? 0?10000200?2?12011?? {12}??1010000 0102001100 010120000? 0300010010 {01}00211?11? ?1???20??? 00?1?10?1? 0?00?1?01? 0100 121111 ?000100100 2101111111 1121112?

Dyrosaurus phosphaticus
1010000?10 001101002- 1111000-01 ?21021112? {12}101010011 0101000000 11?1200001 0300011020 101211?110 211?220011 0001110011 0?01?????? 01?0 ?21111 1000???10? ?001?11??? ?12?0-??

Notosuchus terrestris
2000000?11 1201001011 0?1?001000 0101101210 1100110120 120??0001? 12-00-1201 ?001010{01}21 000-11?000 1101121211 01?0012100 100000?12? 10?0?1011? ??0??????? ?????????? ????????

Malawisuchus mwakasyungutiensis
{34}0000{12}0?10 ?101001001 001?0-1000 ??011012?? 11?0?101{12}0120100001? ???01012?1 ?100010{01} {12}? 00?-1????0 ?10??21111 01??01??00 1?00000012? 101 0?1011? ?00?????00 ????1??0?1 1{12}0010??

Araripesuchus gomesii
3000020?20 01?111100? 0011011010 11010-1200 2100110020 101100000? 12-00-0111 0011010220 001-11?12? 11?112?11? 00???101?0 000001?12? 01?0?1112 ? ?00???????? ?????????? ?1???0??

Baurusuchus pachecoi and Baurusuchus salgadoensis
30000?0??0 1101101010 0011111010 {01}1110-0210 1100110020 001100001? 1??0201111 0(13)11010220 0 0{01}-?1?12{01} 11??12?111 01??012100 011001?12? 0000?1110? ?????????? ?????????? ????????

Goniopholis simus
10100?1??0 0001000?0? 0{23}110?12?0 ?2?12112?? {12}1?1010001 0102000000 1??02000?1 0220110210 001-11?12? ?1???21011 00???10?00 0?1??????? 00?0?? 112? ?0001????? {12}???1????? ?10111{12}?

Sunosuchus junggarensis
10100?0?{12}? 0101010201 0{23}110?1?00 021111122 0 2110010011 0102000000 0100200041 0320100211 0 01-11112? 1101221111 00?1010100 0010011011 0010 111121 ?000?00101 2001111?11 01111111

Eutretauranosuchus delfsi
10100?1?{12}0 000101020? 0{23}11001200 12?11112?? {12}1?10100?? ?1????000? ???0??0041 0220111201 001-11112? ?1???21?11 00???10?00 001000?011 0010111112? ??0?1??1?? ????1????? 0?0?????

Trematochampsa taqueti
???00?0??? 1??1010001 001?????01 ?2011112?0 21100 100?? ??0???001? ???021?1?? ?{12}{12}0?????? ????????? ? ?1?1?20??? 0???01??00 01???????1 0????11??? ?000??? ?0? ????11???? ?{12}{01}???1?

Sebecus icaeorhinus
{34}100020?{01}0 0101001011 0011011?01 02012112? ? {12}1?????0{12}? ?011010011 0010210111 ?22001 0010 00{01}-?1?1{12}{12} 1110221111 00?11101?0 0110??1??0 0?11101l0? ?00???????? ????11???? ????????

Bretesuchus bonapartei
31000?????????????????0??????????????2?????????0{12}?? 01101001????02?0111 12200?0020 001–11?121

Downloaded from https://academic.oup.com/zoolinnean/article/149/4/533/2630922 by guest on 31 August 2021

1?????????????1????00110????{12}? 0001??110????????
??????????????????

Juvenile *Hamadasuchus rebouli*
4000020l?0 0?01011111 0010011?01 1201111220 31?
01110?2 ?011010011 0100210?11 1?200??2?0 ?????11?
2? ?1?0221111 0011110110 0110?????? ?????2112? ????
?????? ?????????? ????????

Hamadasuchus rebouli
40000201{12}0 0101001000 0011011101 1201201220
3110111022 1011010011 0100210111 1220000220 00
2-111122 2110220111 0011110?10 ?110??????
??????112? ?????????? ?????????? ????????

Pabwehshi pakistanensis
{34}????????? ?????????? ?????????? ?????????? ????????22
00100?0011 02-020?1?? 1????????? ??????????
?????????? ?????????? 0????????? ??????1??? ?????????? ??
???????? ????????

Stolokrosuchus lapparenti
4010020110 0001011011 0210011101 2201211210 31
10110021 1012110011 0011210141 11210??0{12}0 ?02
?111122 11?1221111 0011111?00 010001??2? 01?1121
11? ?????????? ?????????? ????????

Uberabasuchus terrificus
30000{12}0??2 0101001000 001?01{01}001 12012112?
0 11?0110021 10121?001? ???021011? ?0200???{12}? ?
????????? ????{12}2?1?1 00????0??? 0110?0111? 000111
112? ?000?????? ?????????? ?1??????

Peirosaurus torminni
?0??0?0??2 ?{12}010?1?0? 0????????? ???1??1??? ???????
02? 10121?001? 00102?0?11 ???2?????{12}0 ?????????? ?
????????? ?0??1????0?110????{12}1 ??0??1112? ?????????
? ?????????? ??0?10??

Lomasuchus palpebrosus
?010020?{12}2 0101001001 02100?1?01 12?12012{12}
0 {12}1?01100?? ??????0001 00?02?0?11 ?2200??220 ?0
2?111122 1??????1?1 ?0??110?00 0??0????{12}? ??????1
12? ?????????? ?????????? ????????

Mahajangasuchus insignis
?????????? ?????????? ?????????? ?????????? ?????????? ??
???????? ?????????? ?????????? ?????????? ?????????? ????
?????? 011?11??{12}1 0100??1??? ?000100?01 2001111
112 110010??

Theriosuchus pusillus
40100?0?{12}? 1?01010001 02?10?1110 02?1111??? {1
2}11??11101 01020?000? ???01?0021 ?{23}200??2{12}0
{01}0{12}1???1{12}? ?1???21111 00????010? 0?10?0????
0????1112? ?1011???01 2????110?? 11011002

Hylaeochampsa vectiana
??110?0?22 1101010201 03?1001??0 ?2010-1101
21?0010??? ?????????? ??????????1 03?0000120 301{12}0
11121 21??221111 0001011?10 ?????????? ??????1??? ??
???????? ?????????? ????????

Leidyosuchus canadensis
3010010020 0101001200 0211001100 1211201201 21
10010011 0102000001 1000200031 0320000120 3112
011121 310?220111 00?0010110 0-10011110
0101101l2? ?1110??1?? 20?11??1?? 02000-1?

Crocodylus porosus
3010010020 0001011210 0311001220 0211101201 21
10010010 0102000000 1100200041 0320010110 3011
011121 2100220111 0010010110 0111111011 010110
1120 0111000101 2001111112 02000-02

Alligator mississippiensis
4010021022 1201011200 0210011100 1211101211 21
10010010 0102000001 1110100021 0320001220 3122
111122 3100220111 0010010110 0110111120 011110
1120 0111001101 2001111112 02000-01

APPENDIX 4

NODE RECONSTRUCTION

List of node reconstructions for phylogeny illustrated in Figure 9. Each node is reconstructed with unambiguous and ambiguously optimized character-states with delayed transformation. Ambiguously optimized character-states are presented in italics. Character-states unique to each node are presented in bold.

Ingroup clade
1(3), **14(1)**, 35(0), **70(1)**, 79(1), **86(1)**, **93(0)**, **100(1)**, **128(1)**, **138(1)**.

Thalattosuchia
1(0), 3(1), 6(0), *19(1)*, 21(1), 24(0), *31(1)*, **32(0)**, 34(0), **42(2)**, 49(0), 51(0), 52(1), 68(0), *72(1)*, 98(0), **99(0)**, 110(1), 114(1), 124(1), *126(2)*, **141(1)**, **147(0)**, *148(1)*, 151(0).

Steneosaurus (Metriorhynchus, Geosaurus)
27(0), *62(1)*, 94(0), 101(1), 104(1), 127(0), 130(1), 135(0), ***136(1)***, *137(1)*.

Downloaded from https://academic.oup.com/zoolinnean/article/149/4/533/2630922 by guest on 31 August 2021

Metriorhynchus, Geosaurus
5(1), *12(1)*, 46(1), 54(0), 59(0), **119(0)**, *131(1)*, **139(1)**, **141(0)**, **143(1)**, **145(0)**, **149(0)**, **152(0)**, 157(0), **158(0)**.

Metasuchia
9(1), *12(1)*, 17(1), **23(1)**, *37(1)*, **38(2)**, *41(1)*, *45(1)*, 46(1), **49(2)**, 79(2), 91(1), **92(1)**, **96(2)**, **97(1)**, **106(1)**, *118(1)*, **153(0)**.

Notosuchia
15(0), *20(1)*, 35(1), 48(1), 52(2), 67(1), **68(2)**, 102(1), **111(1)**, **121(1)**, 127(0).

Araripesuchus [Baurusuchus (Sebecia, Neosuchia)]
26(1), **53(1)**, **69(1)**, 73(1), **78(2)**, 83(1), **89(2)**, **116(1)**, **129(2)**.

[Baurusuchus (Sebecia, Neosuchia)]
51(0), *65(2)*, *72(1)*, 112(1), 113(1).

Sebecia, Neosuchia
15(0), *20(1)*, **28(1)**, 32(2), ***36(1)***, *41(2)*, **43(1)**, 50(1), *72(2)*, **73(2)**, ***87(1)***, ***90(1)***, **95(2),** *104(1)*, ***117(1)***, ***125(1)***, ***146(1)***.

Neosuchia
3(1), *16(1)*, *17(0)*, **18(2)**, 22(2), 26(0), *35(1)*, **40(1)**, 45(0), 49(1), 52(1), 53(0), 54(2), 59(0), 62(1), 68(0), **69(2)**, 72(3), *119(1)*, *140(1)*, ***144(1)***, *148(1)*

Goniopholis, Sunosuchus, Eutretauranosuchus (Dyrosaurus, Pholidosauridae)
1(1), 12(0), 28(2), *33(1)*, **44(1)**, *69(4)*, 75(1), 79(1), 112(0), *118(0)*, 123(1), 130(1), 154(1), 156(1).

Dyrosaurus, Pholidosauridae
6(0), **13(1)**, 18(0), 27(0), 38(1), 43(0), 64(1), 69(0), 73(0), 75(0), 78(0), 81(1), *84(2)*, **89(1)**, *90(0)*, 97(0), *98(0)*, 109(1), 113(0), 122(1), 126(2), 129(1), **153(2)**.

Pholidosauridae
4(1), 15(1), 24(0), *31(1)*, 49(0), 50(0), **57(1)**, **58(1)**, 142(1).

Crocodylia
9(2), 17(1), 20(0), *33(1)*, 36(0), 81(3), *94(0)*, 97(0), 103(1), 104(0), 109(1), *122(1)*, 124(1), 126(0), 132(1), **133(1)**, 134(1), 135(0), *150(2)*, 151(0), **152(2)**, 155(0).

Alligatoroidea
31(1), 60(1), 76(0), **82(1)**, *84(2)*, ***91(3)***, 120(0).

Sebecia
60(1), 61(0), **71(1)**.

Sebecidae, Peirosauridae
6(2), *30(1)*, *35(2)*, **56(1)**, 62(0), **66(1)**, *93(1)*, *105(1)*, *124(1)*.

Sebecidae
2(1), 78(0), 129(0).

Peirosauridae
8(1), *31(1)*, *39(1)*, *51(1)*, 83(2), 90(2), *103(1)*

Stolokrosuchus, Lomasuchus, Uberabasuchus, Peirosaurus
10(2), 24(0), 54(2), 55(1), *63(1)*.

Downloaded from https://academic.oup.com/zoolinnean/article/149/4/533/2630922 by guest on 31 August 2021